2013-06-13

Miniaturized Electrostatic Ion Beam Trap Mass Analyzer

Junting Wang
Brigham Young University - Provo

Miniaturized Electrostatic Ion Beam Trap Mass Analyzer

Junting Wang

A thesis submitted to the faculty of
Brigham Young University
in partial fulfillment of the requirements for the degree of

Master of Science

Daniel E. Austin, Chair
David V. Dearden
James E. Patterson

Department of Chemistry & Biochemistry

Brigham Young University

June 2013

ABSTRACT

Miniaturized Electrostatic Ion Beam Trap Mass Analyzer

Junting Wang
Department of Chemistry and Biochemistry, BYU
Master of Science

The electrostatic ion beam trap (EIBT) was designed by D. Zajfman during the previous decade. This ion trap combines many properties of the Fourier-transform ion cyclotron resonance (FTICR) mass analyzer and time-of-flight (TOF) mass analyzer. There are several advantages for the electrostatic ion beam trap. First, large mass-to-charge particles in an electrostatic field could be easier to analyze. Second, there is a folded flight path, which could make the mass analyzer smaller compared to conventional TOF mass analyzer. This principle of operation of this ion trap is analogous to an optical resonator. The ions are trapped in a voltage valley and oscillate between the two parallel sets of mirror electrodes with high voltages.

In this thesis, I first describe a new type of miniaturized electrostatic ion beam trap mass analyzer that consists of two printed circuit boards (PCBs). The facing surfaces of these boards are imprinted with copper electrodes. The center of the boards is field free and at ground potential with ion mirrors and Einzel lenses on either side. A charge detector is attached to the center for recording the time-dependant motion of the ions in the field. The PCB-based EIBT design is easier to construct than the original EIBT mass analyzer. The electrostatic fields are optimized by adjusting the potential on the mirror electrodes as well as the geometry of the electrodes. Although nondestructive charge detection is much less sensitive for small ions, this detection is ideal for analysis of large ions. The planar electrostatic ion beam trap is inexpensive, small, and simple to operate. The PCB EIBT device was designed, built, and tested using metal samples such as copper and nickel. The electric field of the PCB EIBT is not the same as that of the original EIBT. Unfortunately, there were no ion signals captured in image charge detector.

Another new type of miniaturized electrostatic ion beam trap was made by depositing electrodes onto Kapton film. Seven thin tin/copper traces (1 mm wide by 0.015 mm thick) were deposited onto each side of a flat, flexible circuit board substrate (Kapton film 0.15 mm thickness). The film was rolled to form a cylinder. The flexible EIBT is small (4.5 cm × 8 cm), and lightweight (~1 g). This device was tested using laser ablation of CsI. The CsI signals were detected by the charge detector, amplified and sent to the oscilloscope. Fourier transformation was used to convert the data to the frequency domain spectrum. The resolution of Cs^+ is around 1000 ($m/\Delta m$) from initial flexible EIBT test. The mass accuracy of the Cs^+ peak is better than 0.1%.

Keywords: Miniaturized electrostatic ion beam trap, Kapton film, charge detector

ACKNOWLEDGMENTS

My dissertation and research cannot be completed without the help and support from many people. Now I would like to give my sincere appreciation to all of them.

First of all, I would like to offer my deepest appreciation to my advisor, Dr. Daniel E. Austin, for his patience, guidance, encouragement, and support in all aspects of my scientific education. I am very grateful to have had the opportunity to work under his supervision. He teaches me how to be a professional scientific researcher and helped me in the writing of this thesis.

Furthermore I thank my dedicated and willing graduate committee members Dr. David V. Dearden and Dr. James E. Patterson for their encouragement, insightful comments and those hard questions. Bart Whitehead, Robert Hallock and Keith Kling, the Chemistry department instrument technicians, have been helpful with me to fix any instrument problems. I thank Therin Garrett of the BYU precision machining laboratory. He helped with the machining part of my project.

I also thank my dear colleagues Brandon Barney, Ying Peng, Sara Pratt, Nick Taylor and Zhiping Zhang, and for their superior assistance and guidance that they were always so willing to provide. They provided me such a great research group which will lead me to success.

My parents are always lightening my life with love and guidance. I most graciously thank my wife, Changna, for more than ten years' continued love, devotion and support. Her support for my education will always be appreciated. Our baby cutie, Weiwei Wang, brings me unlimited happiness. Her birth taught me how to be a father and the need to take responsibility for my family.

Last but not least, I would thank the Department of Chemistry and Biochemistry at Brigham Young University for providing me the opportunity and financial support for my graduate study. I also acknowledge the funding support from NASA Planetary Instrument Definition and Development Program.

Table of Contents

List of Figures

List of Tables

Chapter 1: Review of Electrostatic Ion Beam Trap

1.1 Introduction

Mass spectrometry is a very important technique and has been applied to atomic physics, reaction process monitoring, chemical analysis, and thermodynamics, among other fields. It developed very rapidly during the last decade due to various ionization and trapping techniques improved. The mass analyzer is the most important part of a mass spectrometer. It is used to trap ions in static electric and magnetic fields or time dependent fields. Researchers found that electrostatic storage devices could work as mass analyzers in the 1990s.[3-4]

Electrostatic storage devices were originally used to store electron beams for physics research. Since then, physics research involving ion storage has evolved into a mature field. The ASTRID (Aarhus Storage Ring in Denmark) was first designed in 1985 by the Institute for Storage Ring Facilities in Aarhus.[5] The large-scale ring was to store low-energy heavy ions for laser spectroscopic and laser cooling experiments and atomic collision studies. However, they found it could possibly store the energetic electron beams in the ring and operate as a synchrotron radiation source. The Danish electrostatic storage ring for ions (ELISA) was set up in 1998.[6] (Figure 1) It was the first electrostatic storage ring in the world. The second ELISA was built in Japan by the T. Tanabe group.[7] They used cylindrical deflectors instead of the spherical deflectors that were used in the first ELISA. The change avoids a narrow focus of the ion beam and an unwanted loss of ions. These rings could store a beam with well-defined kinetic energy and direction, allowing highly-efficient detection techniques. ELISA enables the storage of low-energy, heavy ions for a long period of time.[8] The stored ions could interact with laser light and

low-energy electrons which could be used in the study of photo-, bio-, cluster, and molecular physics. However, they are large, expensive and require accelerators to produce the ion beams. Some researchers thought it was necessary to develop small electrostatic devices.[9-10]

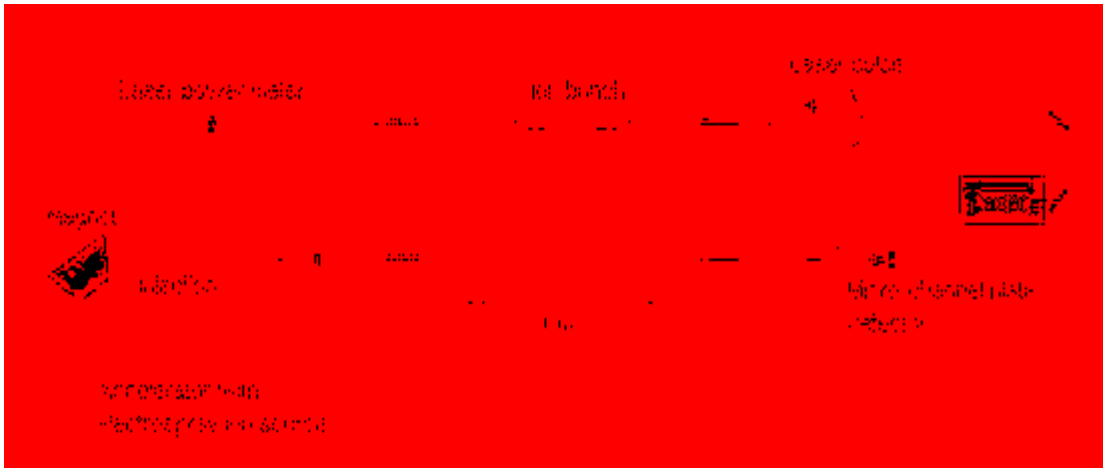

Figure 1. Schematic diagram of the electrostatic ion storage ring ELISA

1.2 Early Electrostatic Ion Beam Trap

L. Andersen, O. Heber and D. Zajfman first described a new type of linear electrostatic ion beam trap in the 1990s.[11-12] The EIBT (electrostatic ion beam trap) stores and manipulates ions with only electrostatic fields. The ions oscillate in the trapping region of the EIBT. Two series of electrodes on two sides of the ion trap are called electrostatic mirrors. (Figure 2) The EIBT looks like a multiple reflection time of flight mass analyzer. It is simple to operate, and has good resolution and sensitivity. Compared to the traditional ion traps such as the Penning trap or the Paul trap, the EIBT does not need to work with magnetic fields or RF electric fields.

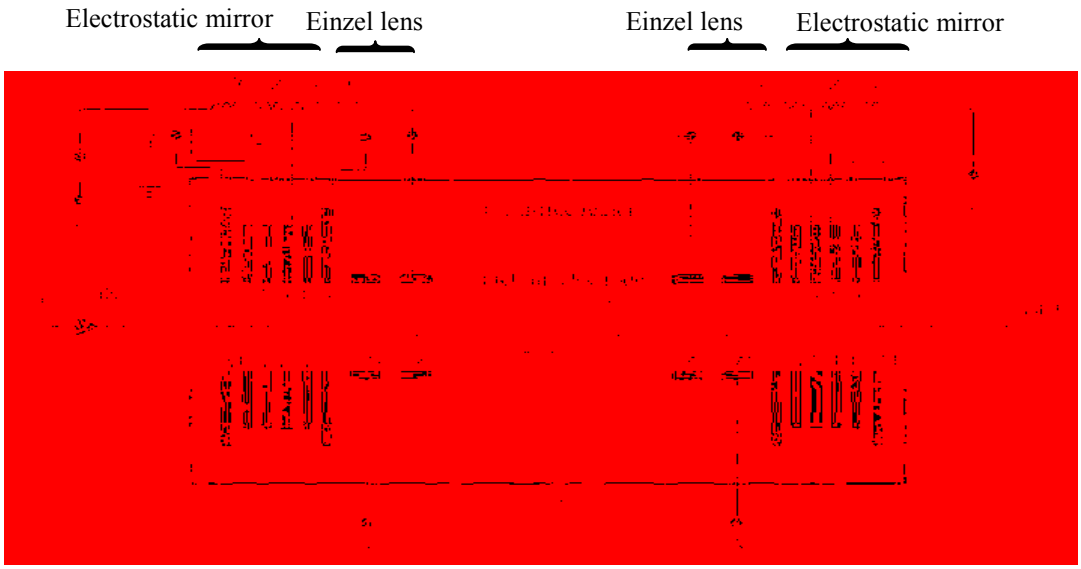

Figure 2. Zajfman's EIBT diagram.

The ions are injected as a packet from the entrance (left) side of the EIBT. The right electrostatic ion mirror has applied high voltage 5000 V on A1. The ions decelerate after they pass the field-free region until the velocity is zero. They turn around and are reaccelerated by the electric field of the ion mirror, now moving left. They oscillate in the trapping region, and neutralized ions are produced in charge-exchange collisions with the residual gas. The number of the neutralized ions could be measured by microchannel plate detector. The Einzel lens consists of electrodes Z2, Z1 and E1. The Z1 electrode was set to 3500 V (V_z) and the others were grounded. The electrostatic mirror consists of E2, E3, E4, E5 and A1 (V_s).

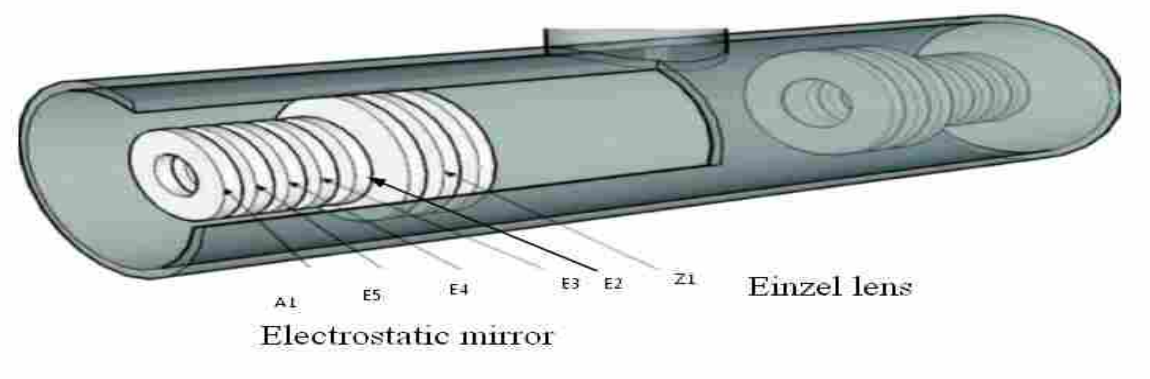

Figure 3. A 3D overview of Zajfman EIBT.

The electrostatic mirror in Zajfman's EIBT consists of five electrodes E1, E2, E3, E4 and E5 (Figure 2). The voltages on these electrodes linearly increase from 1000 V to 5000 V. Electrode E1 is grounded, while electrode E5 is V_s (5000 V). One potential valley is created when the two mirrors switch on. It confines the ions in the longitudinal direction. An asymmetric Einzel lens on either side consists of three electrodes (E1, Z1 and Z2) which are used to focus the ion beam in flight. The electrode Z1 potential is equal to V_z (3500 V) while the E1 and Z2 electrodes are grounded. An additional grounded electrode (A1) closes the stack of electrodes to reduce the electric fields outside the trap. The ring pick-up electrode for charge detection is shown in the center of the trap which is field free and at ground potential (Figure 3). The ions' various frequencies and their relative abundances can be extracted mathematically by using a Fourier transform, which converts a time-domain signal to a frequency-domain spectrum. The microchannel plate detector located at the end of the trap measures the number of neutralized ions through the exit mirror. These neutralized ions were produced in charge-exchange collisions with the residual gas in the EIBT.

The physical principle of the EIBT is very similar to an optical resonator, which can "trap" photons. Photon optics and ion optics are equivalent in many ways. The EIBT works according to the same principle as for an optical resonator for two equivalent concave mirrors. The stability criterion of an optical resonator is related to the focusing properties of the mirrors. By using methods such as ray transfer matrix analysis, we can calculate the stability criterion[11, 13]

$$0 \leqslant \left(1 - \frac{L}{R_1}\right)\left(1 - \frac{L}{R_2}\right) \leqslant 1. \tag{1}$$

For a resonator, two mirrors have radii of curvature R_1 and R_2 and L is the effective distance between two mirrors. When $R_1 = R_2 = 2f$ (the focal length of the mirrors) (Figure 1.4), the equation (1) is equivalent to

$$\frac{L}{4} \leqslant f \leqslant \infty \tag{2}$$

Thus, the stability condition (for a beam in the axis of the trap) requires the focal length of the mirrors to be larger than or equal to one quarter of the trap length. Second, the value of the maximum potential on the mirror has to be high enough to confine the ions longitudinally. Therefore, the ions can be trapped in the electrostatic field.

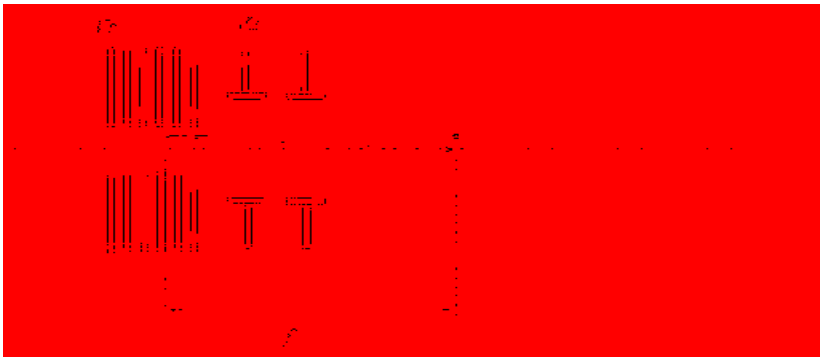

Figure 4. Focal length (f) is the distance between ions turning point and the center of the EIBT. Focal length (*f*) is the distance between ions turning point and the center of the EIBT. V_s represents the highest voltages in the electrostatic mirror. V_z represents the potential on the Einzel lens.

The ions stored in the trap oscillate between these two cylindrically symmetric electrostatic mirrors with motion frequencies that are proportional to the square root of the charge-to-mass (z/m) ratio:

(3)

The mass of singly charged particles can be obtained by measuring their oscillation frequency; for multiply charged particles their charge has to be measured by an image charge detector, which is located at the center of EIBT. The mass detection range of the EIBT is unlimited. Collisions between ions and background gas molecules will limit ions' flight length in the trap. The resolution of the EIBT will depend on the numbers of cycles

of the trapped ions. The sensitivity of the EIBT is related to the detection limit of the image charge detector and how the ions enter the trapping field.

1.3 Zajfman's EIBT

The Zajfman EIBT design was very simple. The entrance mirror electrodes (E1, E2, E3, E4, E5) of the EIBT are on the left, and the exit mirror electrodes are on the right. Einzel lens electrodes (E1, Z1 and Z2) are at both ends to focus ions. The charge detector consists of a pick-up electrode in the center of the trap, which is a field-free region. The microchannel plate detector is located at the exit side to measure the number of neutralized ions.

The voltage gradients on the electrostatic mirrors are important to trap the ions. The condition $qeV_s > E_k$ has to be fulfilled,[11] where q is the charge of the ions and E_k is the ions' kinetic energy. V_s is the maximum potential on the electrostatic mirror. The focusing potential V_z on the Einzel lens determines the focusing length of the ion trap, which can be computed by simulated ion trajectories. If the ion beam kinetic energy is 3.5 keV singly charged and V_s = 5 kV, V_z is valid between 2.9 kV and 3.3 kV. In the EIBT case, the field changes according to the kinetic energy of the trapped ions.

The first version of Zajfman's EIBT was 407 mm long (Figure 3). The mass resolution ($m/\Delta m$) has been demonstrated to be more than 10^5 for several isotopes of Xenon.[9] The high mass resolution is because the ions were clustered in Zajfman's ring electrode EIBT design and could oscillate in the Zajfman EIBT. The image charge detection method has better resolution for large ions compared to the conventional types of time of flight MS and Fourier transform ion cyclotron resonance (FTICR) MS. It offers an alternative for measuring the charge and the m/z of the high mass ions. The

central field-free part of the trap can be made as short or as long as needed. The ions travel in straight lines according to their kinetic energies. The ion beam was produced by electron impact ionization. Dr. Zajfman set up defocusing and magnetic steering to distort Xe isotopes relative abundance.[14] The ion beam energy was set to 4.2 keV and about 10^6 ions were injected. The EI source produces a constant current of ions, which was chopped by applying a ~5 μs electric pulse to the entrance electrostatic mirror. The potential valley was immediately established to trap ions. The lifetimes of stored ions were recorded by a microchannel plate detector (MCP), which is behind the exit electrostatic mirror of the EIBT. The trapped ions capture electrons from the residual gas and then turn to neutral particles, which are no longer trapped. These neutral particles exit the trap and travel to hit the MCP detector. The ions' lifetimes and the total number of stored ions could be measured. It is important that the space charge effects limit the number of stored ions but they did not account for it. The number of stored ions N_t is a function of the injection particle current I and the oscillation period T, and is given by $N_t = IT$. The lifetimes were found to be proportional to trap pressure and also related to the velocity of the ions.[11]

(4)

n: Residual gas density

v: Beam velocity

σ: Cross section for electron capture (10^{-15} cm^2 for all the ions they test)

1.4 Current EIBT application

The most important feature of the EIBT is that it has no upper mass limit. It is simple to operate, has good resolution and has no magnetic fields. A lot of research groups are interested in applying it in biological sample analysis, electron collision and metastable ions lifetime study.[15-17]

The EIBT could be used for collision studies, metastable ion lifetime measurement and biological ion measurements. Mary Rodgers at Wayne State University studied collision-induced dissociation (CID) of Na^+(xBA) complexes and six other sodium cationized MALDI matrices (nicotinic acid, quinoline, 3-aminoquinoline, 4-nitroaniline, picolinic acid, and 3-hydroxypicolinic acid) with Xe using ion beam mass spectrometry.[18] The Na^+(xBA) are Na^+ bound to benzoic acid and all mono- and dihydroxy-substituted benzoic acids. They analyzed the affinities of MALDI matrices and binding conformations of Na^+ and MALDI matrices. Their work tried to optimize ionization processes in MALDI. The ion beam MS provides the dissociation time and the cross section of ions in CID. Some papers have been published to describe the measurement of various metastable levels of ion lifetimes with the EIBT. The Zajfman group measured metastable He^-, Be^- and NO^+ ions lifetimes in the EIBT, which avoids magnetic field induced effects.[19] They also measured the lifetimes of three negative molecular hydrogen anions: H_2^-, D_2^-, and HD^-. The real lifetimes of these ions are much longer than the theoretical calculations, possibly because they have more than one electronic state. They also set up a mass selector between the entrance electrostatic mirror and the pick-up electrode, which is located at the center of the EIBT. This mass selection technique could eject undesirable ions. Self-bunching ions could fly longer in the

trapping field.[20] Their signals will not decay so quickly as the signals that are lost because of collision with residual gas. The requirements of self-bunching are dependent on the potentials of the two electrostatic mirrors.

The measurement of biological ions was a challenge for small mass analyzers without an Orbitrap. However, the Orbitrap is hard to machine. It needs an electrostatic field with a quadro-logarithmic potential distribution. It is possible to apply the linear EIBT to the study of biological molecules. Dr. Benner constructed one linear EIBT at Lawrence Berkeley National Laboratory for biomolecule analysis.[17] He used electrospray to inject highly-charged, 2.88 MDa plasmid DNA ions (4.3-kilobase-long circular DNA molecules of a bacterial plasmid) into the electrostatic ion trap. The sample was electrosprayed at approximately 1μl/min with an atmospheric pressure ion source. The ions cycled many times through the detection tube (37.5 mm × 6.5 mm i.d.), which was connected to a low-noise charge sensitive amplifier. When DNA ions entered this detection tube, the image current triggered a circuit that immediately switched on the entrance electrostatic mirror. The ions were trapped as long as 10 ms and cycled 450 times. The resolution ($m/\Delta m$) of the peak at 2.88 MDa was approximately 25. The main reason for low resolution was no sample preparation before mass analysis. The authors believed that sample preparation such as desalting the DNA molecules could improve the resolution in their EIBT. The DNA ions carried more than 250 charges. (Figure 5)

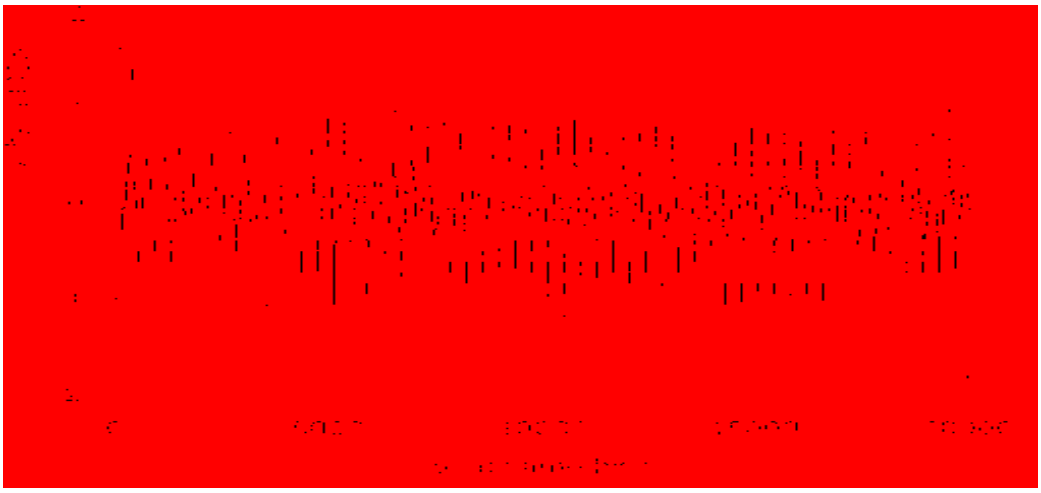

Figure 5. The oscillatory waveform in the figure describes the cycling of DNA ions in the Benner EIBT. The oscillatory waveform in the figure describes the cycling of DNA ions in the Benner EIBT. The vertical scale is in volts, and the displayed trapping time is 1 ms. Ion charges were measured by the height of the peaks, and the time between a positive peak and the ensuing negative peak is the time needed for an ion to fly through the detector tube. Ion mass is calculated. The figure is cited from the Benner paper in *Analytical Chemistry, 1997, 69(20), 4162-4168.*

1.5 Various EIBT Designs in Other Research Groups

Another device, the Conetrap, similar to the EIBT, was developed at the University of Stockholm.[21] In this case, the entrance mirror or exit mirror consists of only one electrode, (Figure 6) whose shape also produces an electrostatic field. The first test for the Conetrap used singly charged argon ions, which were produced in a gas discharge ion source and transported to the trap. The two ion mirrors provided high voltages to keep 4 keV Ar^+ ions moving back and forth in the trap. The MCP was behind the exit mirror to record the ion lifetime. The Conetrap was also used to measure the lifetime of metastable negative helium ions. However, they did not set up an Einzel lens to focus the ion beam and presumably the cone shape provides some focusing functions. The ion dispersion of the turn points could lead to the loss of ions. It was not suitable for mass detection.

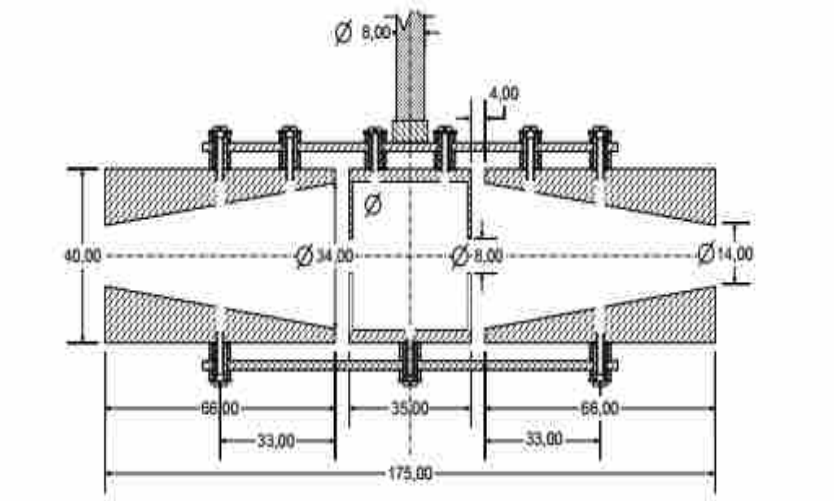

Figure 6. Design of the Conetrap (all dimensions in mm) from University of Stockholm.[14]

Another type of EIBT designed by the Bernard group in France was called the "Mini-Ring".[22] It consisted of four horizontal parallel plate deflectors (D1, D2, D3, D4) and two conical electrostatic mirrors (C1 and C2) (Figure 7). They used three Faraday cups F1, F2, and F3 and a channeltron detector for analysis. The current measurement with F1 is used to tune the incoming beam. The voltages on the deflectors and conical mirrors were adjusted to make the ion beam hit F2 or F3. The lifetimes of Ar^+ and He^+ ions beams were measured in this ring at 10^{-7} mbar.

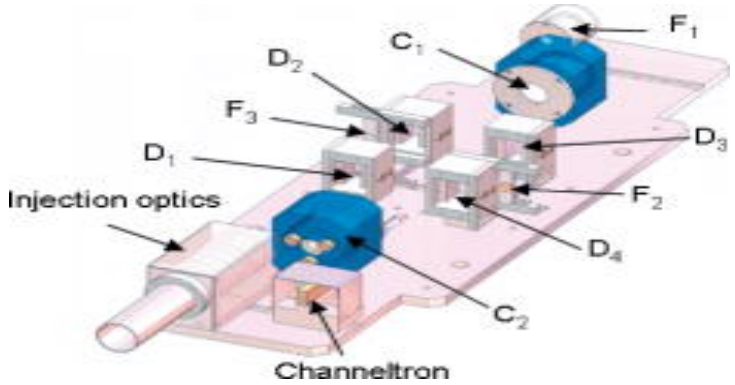

Figure 7. A three dimensional scale drawing of Mini-Ring.The ion optical elements—two conical mirrors and four deflector—are carefully positioned on a common mounting plate.

Ermakov and Hinch developed an electrostatic autoresonant ion trap mass spectrometer in 2010.[23] The novel autoresonant trap mass spectrometer (ART-MS) was constructed from parallel plates alone (Figure 1.8). Mass spectra were generated by an autoresonant pumping mechanism. The ions were created by electron impact ionization. An RF potential was applied to the central electrode. When the oscillation frequency of

the trapped ions is the same as the applied potential, the RF would be the driving frequency in the potential well. It is known as autoresonance. The resonant frequency is mass to charge ratio (*m/z*) dependent. Their ART-MS is very compact (less than 8 cm long), and requires only very small power (in the mW range excluding ionizer) as they use static potentials and a very small RF voltage (below 100 mV_{p-p}). It was operated at background pressures in the 10^{-8} mbar range. They found the RF amplitude has strong effects on the sensitivity and resolution. The resolution of the MS is around 50, dependent on working parameters. (Figure 8)

Chapter two describes the general design and properties of our planar plate electrostatic ion beam trap (EIBT). The planar plate EIBT has good ion beam storage capability but the electric field is a little different from Zajfman's EIBT. I could not achieve any signals from our planar plate EIBT. The flexible EIBT is presented in chapter three. It has better resolution and simple alignment. A Cesium iodide mass spectrum was obtained by Fourier transform. Finally, future work will be presented for our EIBT.

Figure 8. Parallel plate ART-MS during construction.

Chapter 2: Planar Plates Electrostatic Ion Beam Trap

2.1 Introduction

The main goal of my research is to develop a new miniaturized mass analyzer for space exploration to fulfill NASA requirements. First, the new mass analyzer should have high mass resolution. At minimum it should have a mass resolution, $m/\Delta m \geq 500$, which can separate astrobiological chemical species pairs that are slightly different in mass. Second, the instrument should be small enough to fit on a spacecraft. It needs to have low power requirements and be lightweight. Third, the mass analyzer should be robust because it needs to work in a harsh outer space environment such as low pressure (10^{-12} torr), and temperatures up to +470 ^{O}C and down to −180 ^{O}C.[24-25] Finally, it should be compatible with laser ionization, which is used in interplanetary exploration. Based on these requirements, the results from our EIBT design should be demonstrate that it is a suitable mass analyzer for future landing missions.

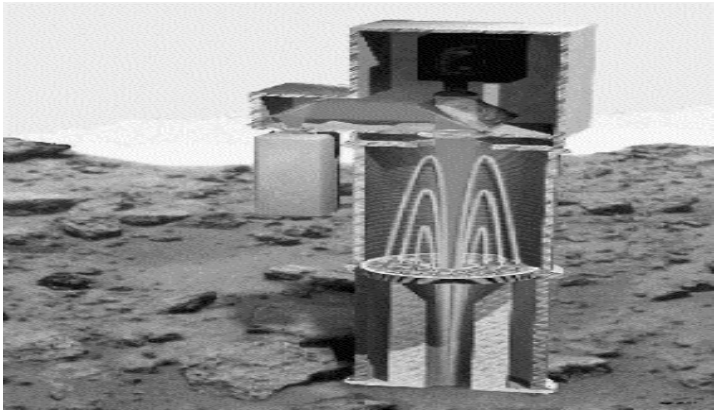

Figure 9. The miniature time-of-flight mass spectrometers for in situ mass analysis. The L2MS (two step laser TOF-MS) with curved-field reflectron and co-focused laser and imager. It was designed by W. B. Brinckerhoff. [1-2]

Small mass analyzers for in situ planetary exploration could be developed such as the L2MS but our group uses printed circuit board (PCB) technology to replace the traditional ion trap hyperbolic surface shape. The printed circuit boards made from laminate material have high temperature and vacuum tolerance. These planar PCB mass analyzers provide the same potential functions in the trapping region as traditional ion traps. This technology has already been used to miniaturize radiofrequency ion traps such as the toroidal ion trap, the Paul ion trap and the rectilinear ion trap. The metal electrodes on the flat surface are covered by a resistive material such as a germanium layer. The potential on the germanium layer can be adjusted by changing the electrode geometry or by changing the voltages. Therefore, the electric fields on the planar plates could be optimized either electrically or physically. Two planar plates make one trap. These are easier to set up than traditional traps. Our planar plate EIBT and Zajfman's EIBT have very similar electrical fields and mass resolution performance.

2.2 Computer Simulation of Zajfman's EIBT Performance

The original Zajfman EIBT[11] has two electrostatic mirrors and an Einzel lens on each side. (Fig 10.a) Each Einzel lens consists of two wide electrodes and the nearest thin electrode. The middle wide electrode will have several thousand volts (V_z) applied to it and the other two electrodes will be grounded. The electric field in X-Y dimensions is shown by the SIMION 7 software, which calculates electric fields based on the voltages of electrodes and ion trajectories in those fields (Fig 10.b).

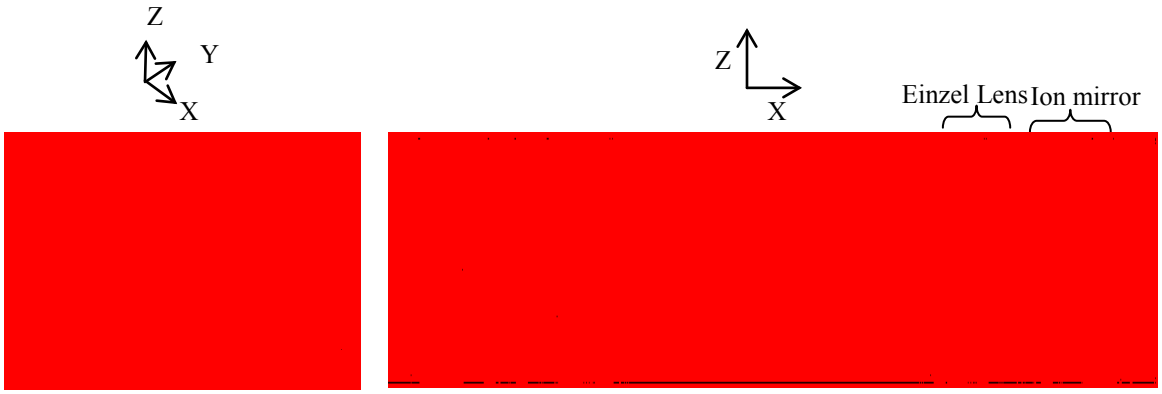

Figure 10. (a) Zajfman EIBT 3D views in SIMION 7. (b) Electric field in XZ view when Vz is 3500 V and the potentials on the ion mirrors linearly increase from 1000 V to 5000 V.

2.2.1 Einzel Lens Function in EIBT

The purpose of the Einzel lens is to focus the ion beam without changing the energy of the beam. The focusing effect is a complicated function of cylinder electrode lengths, voltages and diameters. The following figure is a three-element lens system with the equipotential surfaces having voltage of $V_1 = 0$ V, $V_2 = 3500$ V and $V_3 = 0$ V (Figure 11). The focal length of a monoenergetic ion beam only depends on the potential V_2, and on the size of the lens elements.

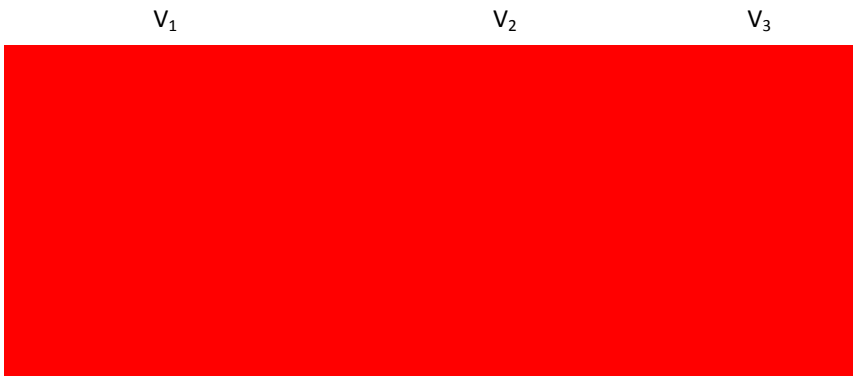

Figure 11. The geometry of a three-element lens which consists of three coaxial cylinders. Two of them have a diameter of 26 mm, separated by a distance of 8 mm. The smaller cylinder's diameter is 16 mm. The distance between the smaller one and the bigger cylinders is 6 mm. The cylinders are at potentials 0 V, 3500 V and 0 V with lengths of 1 mm and 5 mm, patterned after the Zajfman design.

(a). (b).

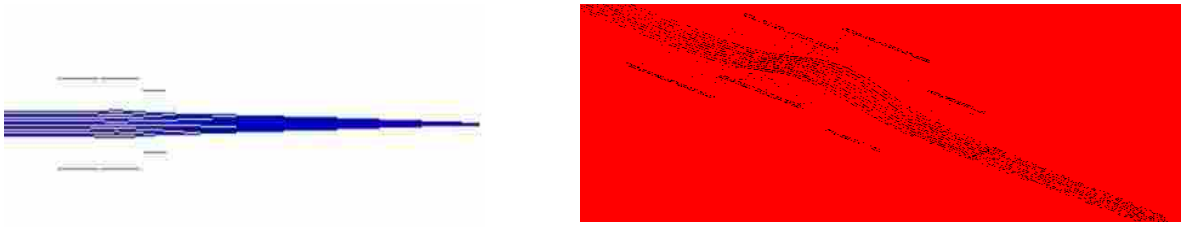

Figure 12. (a). An XY view of an Einzel Lens. A group of positive ions are flown into the lens at initial parallel trajectories and then bend to focal point. (b). The focusing effect is shown in the potential energy map.

The Einzel lens system shown in Figure 12 is created by SIMION 7 based on the Zajfman design. The ion beam is well focused after it flies through the Einzel lens. The

4.0 keV copper ion beams in SIMION 7 flying through the Einzel lens system show the relation between focal length and the potential on V_2 (Figure 13).

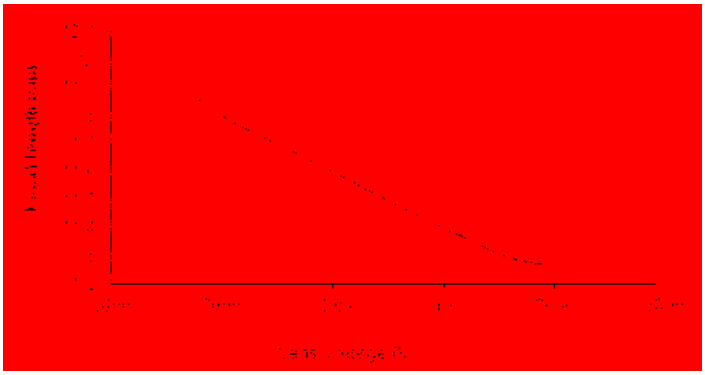

Figure 13. The relationship between focal length and the voltages on the Einzel lens. The focal length depends on the voltages of the Einzel lens.

2.2.2 Ion Trajectory Simulations in Zajfman EIBT

We used SIMION 7 to simulate ion trajectories in the derived electric field using the Runge-Kutta method with the Zajfman EIBT. The electrodes in the trap were drawn with a ring shape. The inner diameter (i. d.) of the five mirror electrodes E1, E2, E3, E4 and E5 are 16 mm and their thicknesses are 3 mm. A larger ID (26 mm) was chosen for the focusing electrodes Z1 and Z2 in order to obtain a smaller aberration in the focal length. The distance between each electrode E is 6 mm, between E1 and Z1 is 6 mm, and between the two Z electrodes is 8 mm (Figure 14. a). The Zajfman EIBT was aligned by ceramic balls and the two sets of electrodes are connected by four rods which guarantee the electrodes are coaxial. The distance between the two A1 electrodes is 407 mm. A1 and Z2 are grounded. Z1 is 3500V but E1, E2, E3, E4, and E5 are 1000 V, 2000 V, 3000

V, 4000 V and 5000 V, respectively. The copper ions' simulated kinetic energy is 4 keV. There are 100 copper ions injected in this simulation. These ions scatter due to space charge effects and residual gas collisions but the Einzel lens focuses the copper ion beam.

One cycle length is around 63 cm and one cycle time is around 5.74 μs for 4 keV copper ions. The copper ions will continue to fly until they collide with background gas molecules, turning them into neutralized ions. The 4 keV copper ions' trajectories are shown in the figure (Figure 14.a). The Y-Z view of the Zajfman EIBT (Figure 14.b) proved that the ion beam is trapped in the electric field.

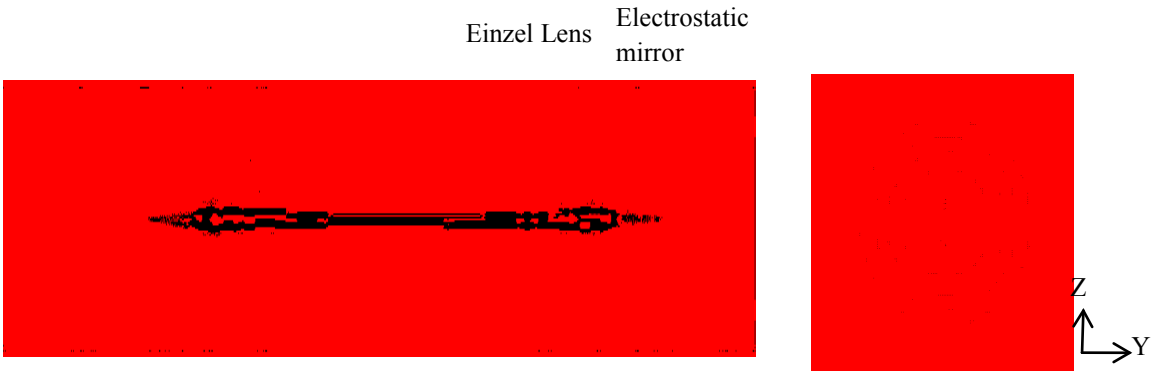

Figure 14. (a) Copper ion beams with 4 keV (green line) were injected in the Zajfman EIBT (XZ view). (b) The YZ view of the Zajfman EIBT showing the ion beam traveling to the trapping region.

2.2.3 Computer Simulation of Planar Plate EIBT Performance

Our planar plate EIBT consists of two parallel printed circuit boards (28 cm × 10 cm), spaced 1 cm apart. The metal electrodes are deposited on printed circuit boards (PCB), and then covered by a germanium layer. The electrode shapes need to match the

equipotential lines of the electric field in the Zajfman design (Figure 15). The center part of the EIBT is the field-free region. It is well shielded and contains the image charge detector.

These two electric fields in the Zajfman EIBT and in the planar EIBT should have almost the same performance in trapping ions. E1 and Z2 (Einzel lens in the trapping electrodes) in the planar EIBT should be at ground potential; Z1= 3500 V, E2 = 1000 V, E3 = 2000 V, E4 = 3000 V, E5 = 4000 V, A1 = 5000 V. The SIMION 7.0 software solves the Laplace equation $\nabla^2\phi = 0$ for a given set of potentials and calculates ion trajectories in the derived electric field. While these potentials are provided, the ions are trapped in the potential valley for hundreds of milliseconds when the vacuum is 10^{-6}~10^{-7} torr. One cycle time is 3.83 μs for 4 keV copper ion and one cycle length is around 41.9 cm.

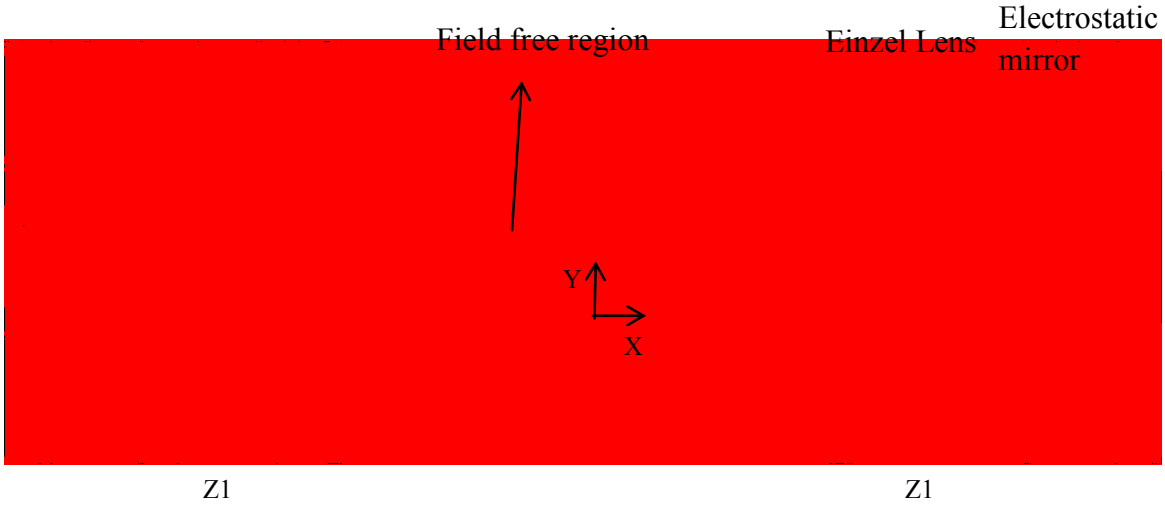

Figure 15. Planar plate EIBT (XY view) in SIMION 7. The voltages applied to these electrodes were the same as for the Zajfman EIBT. The Z1 with focusing potential is 0.5 cm wide in the center and 0.35 cm at the edge. The other electrodes are 0.1 cm wide.

Figure 16. Planar plate EIBT electric field presented in XZ dimension. It is very similar to the Zajfman EIBT electric field.

2.2.4 Electric Field Comparison Between Zajfman's EIBT and Planar EIBT

The differences between the Zajfman EIBT and our planar EIBT are electrode shape and ion trap size. Our planar plate EIBT size is proportionally decreased from Zajfman's EIBT. Our EIBT electrode shapes need to match the equipotential lines of the electric field for the ring electrodes. Therefore, their electric field should be as similar as possible. However, the X-Z view of the electric field in our EIBT is elliptical in shape while Zajfman's EIBT electric field is round. (Figure 17 & Figure 14 b) The potential functions of our planar EIBT are presented in Figure 16. The 4 keV copper ions could be trapped in the center of the electric field but their cycle length is slightly longer than the cycle length in the same size ring electrode EIBT design according to SIMION 7 simulation.

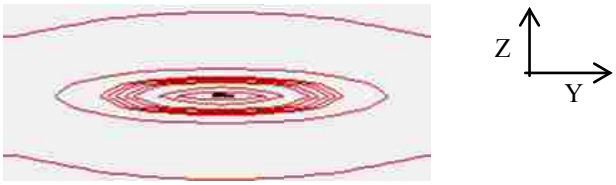

Figure 17. Electric fields in YZ view of our planar EIBT**.**

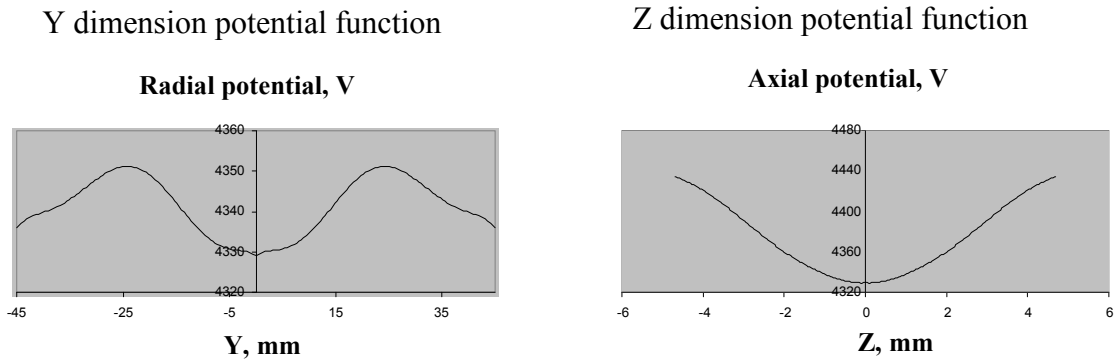

Figure 18. Potential functions in Y dimension (left) and Z dimension (right) in the center of the planar EIBT Einzel lens. The focusing potentials on each electrode are the same as the Zajfman setup. The ion beam could be focused when it passed through the Einzel lens.

During the simulation work in SIMION 7.0, we found that a series of parameters affect the electric field. For example, such parameters included the potentials changing on the electrode, the shape of the metal electrodes and the size of the ion trap. We found that ions with the proper injection angle can be trapped for more time and have a longer flight length due to the potential functions. The injection angle affects the ions' trapping efficiency and capacity in the EIBT. More than 90% of the injected ions could be lost or their flight length decreased in the trapping region because of the injection angle. Our planar EIBT presented better sensitivity than Zajfman's EIBT and more ions could be trapped. The injection angle range of the planar EIBT is larger than Zajfman' EIBT. The miniaturized planar plate electrostatic ion beam trap needs high electric field accuracy.

This accuracy will depend on the shape of electrodes on the EIBT. The potentials on the electrodes of the EIBT could be optimized using SIMION 7.

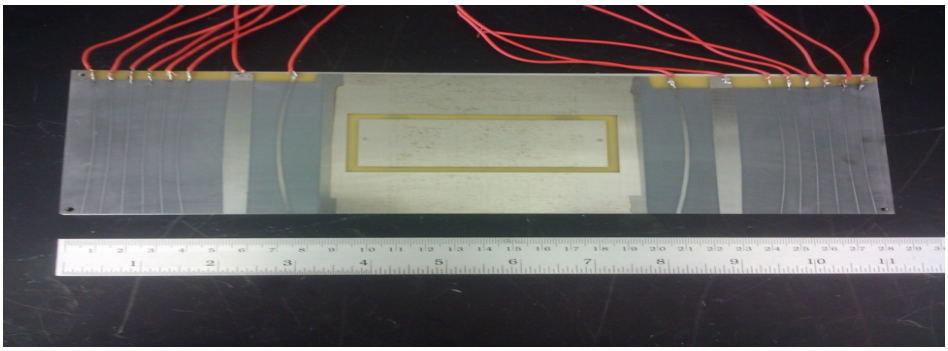

Figure 19. Top-view photograph of a printed circuit board (28 cm × 10 cm) for our EIBT. The 200 nm germanium layer covers the surface of the board except the central region.

2.3 Planar EIBT Experimental Set-up

One planar plate EIBT was set up in our lab using two parallel printed circuit boards (28 cm × 10 cm), spaced 1 cm apart (Figure 19 & 20). Eagle software (Cadsoft) helped us to design electrodes on printed circuit boards. The printed circuit boards were produced by Quickturn Circuits (Salt Lake City, UT). The printed circuit boards are low cost and easy to set up. A 1 cm plastic spacer was mounted between the trapping plates. The facing surfaces of the boards are first imprinted with sets of copper electrodes. Appropriate DC potentials (1000 V ~ 5000 V) are applied to each electrode to allow trapping. Resistors are connected to separate voltages on each electrode. The 200 nm resistive germanium layer was used to cover the electrode space on the boards in order to

avoid unwanted charge buildup and allow the potential to drop smoothly. The new EIBT is a very open structure. Ions can enter the trap through the spacing between two boards. The operating pressure of this device is in the range of 10^{-6}-10^{-7} Torr.

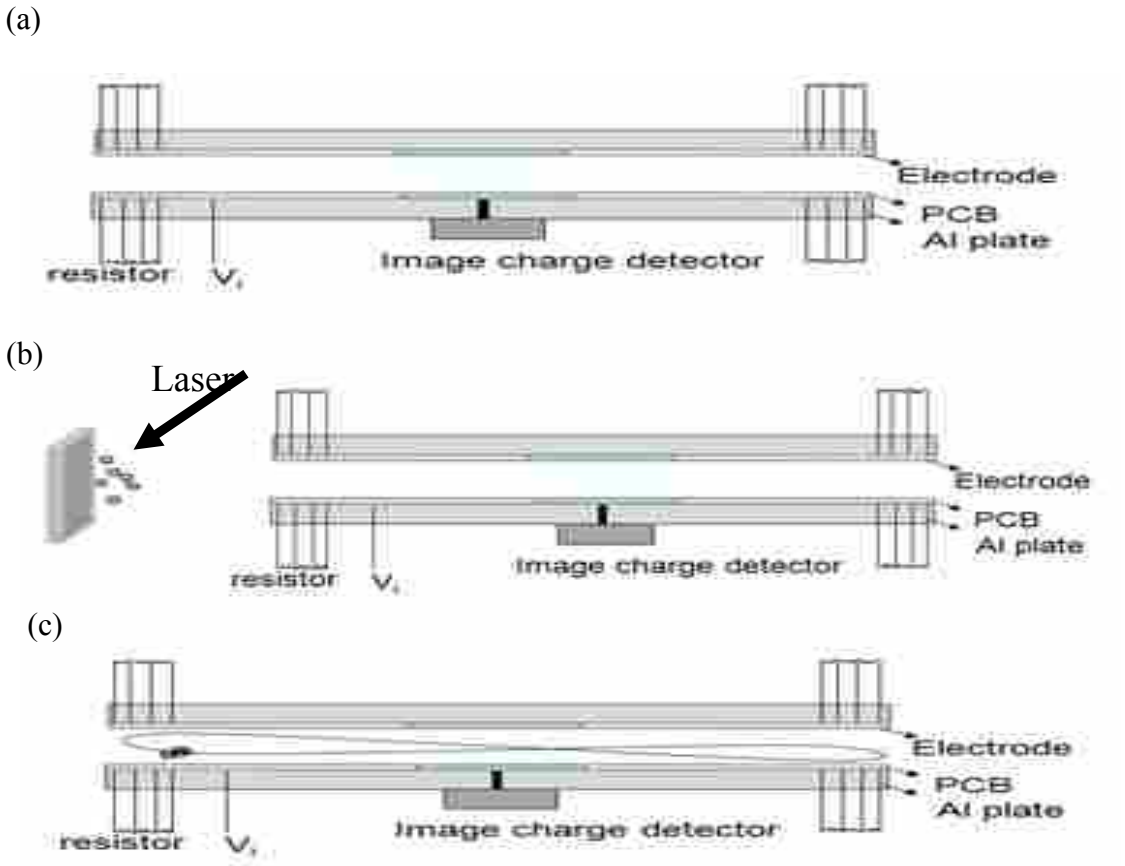

Figure 20. Planar plate electrostatic ion beam trap. (a) It consists of two parallel printed circuit boards (PCB) that are mounted on an aluminum plate. The inside surface of each board is patterned with metal electrodes and overlaid with germanium; (b) in situ laser ionization; (c) The ions are trapped between two PCBs and frequencies are recorded by the image charge detector.

The facing surfaces of printed circuit boards were imprinted with several copper electrodes. The center of the boards is field free (8 cm × 4 cm) and at ground potential. A charge detector is connected to the field free region. The design is easier to construct than the Zajfman EIBT mass analyzers. Electrostatic fields can be optimized by adjusting the potentials on the mirror electrodes or by adjusting the geometry of the electrodes. The EIBT mass analyzer could be used for large molecular weight ions such as DNA[17] because of image charge detection and the ions' multiple passes through the trap. Our planar electrostatic ion beam trap combines the advantages of ion traps (inexpensive, small, and simple to operate) with other advantages such as high mass resolution.

2.3.1 Laser Ionization with Copper Plate

In front of a copper target plate, there is a nickel mesh to help ions fly into the ion trap with the same kinetic energy. (Figure 21) The electroformed nickel meshes are manufactured by Buckbee-Mears St. Paul. The mesh has 88% transmission which is suitable for our current experiments. The high ion transmission will help us get more ions

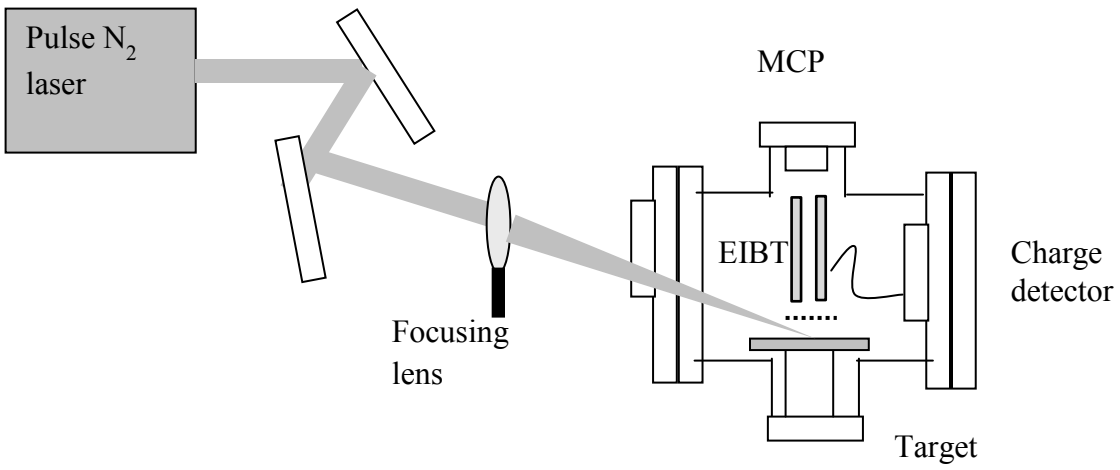

Figure 21. Planar EIBT Experimental Set-up.

to enter the analyzer, which increases the sensitivity of the EIBT. The copper target plate has an active area of 3.5 cm^2 for laser ionization. The surface of the copper plate was cleaned by methanol twice. Sandpaper was used to polish the surface. A pulsed nitrogen laser at a wavelength of 337.1 nm (model NL100, Stanford research) with a pulse width of 4 ns was focused onto the copper target plate with a repetition frequency of 20 Hz. The output energy of the laser was 170 μJ. Using a bi-convex lens with a focal length of 25 cm, the laser beam was focused to the smallest possible spot size, estimated to be 15 μm. We could also use the laser ionization method to produce ions of large molecules such as peptides and proteins.

2.3.2 Image Charge Detection

An image charge detector was used to obtain the ions' frequency in the EIBT mass analyzer and was successfully tested. It is located at the center of the EIBT, which is the field-free region. The traditional charge detector consists of one metal cylinder and one shielded box containing the electronics. The box contains one charge sensitive preamplifier, and three differentiating charge amplifiers on two circuit boards inside the box. The charge sensitive preamplifier is an Amptek (Bedford, MA) A250 on one PC 250 circuit board. Three Amptek A275 amplifiers are on the PC275 circuit board. The preamplifier and amplifier are shielded in the copper box. Initial testing of the A250 and amplifier was done with an arbitrary waveform generator and a power supply for the A250. With the oscilloscope trigger using the waveform generator signal, the amplified A250 signal was observed to have the same frequency as the waveform generator with averaging at 100 sweeps. While testing in vacuum, multiple signals were obtained

(Figure 22). When we increased the amplitude of negative pulse peak (pink), the peak (yellow) amplitude from the image charge detector also increased proportionally.

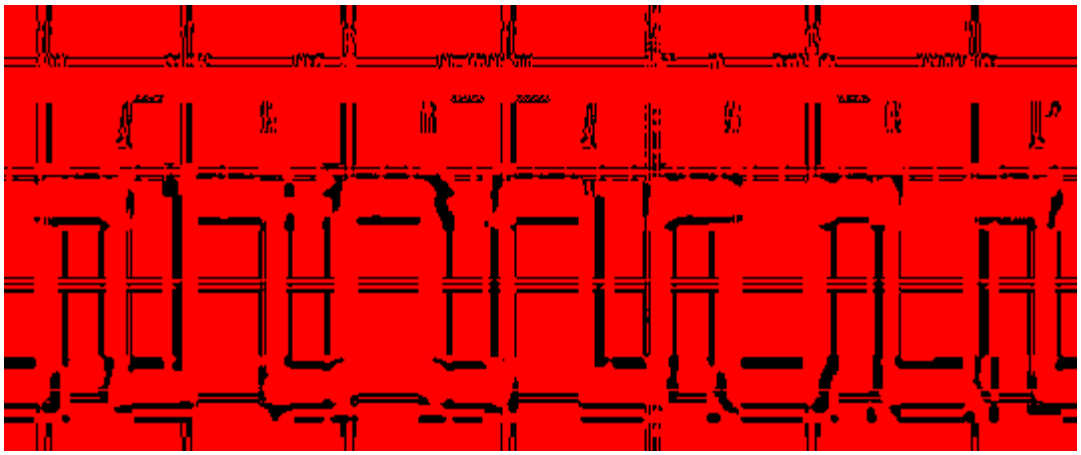

Figure 22. Charge detector signals (yellow) with negatively pulsed (pink) by waveform generator. The axis is 100 mv/div for charge detector signals, and 1V/div for the waveform generator pulse. The frequency is 5 kHz.

The time between negative and positive peaks approximates the time required for the particle to pass through the field free region and can be used to calculate the particle velocity. The areas of the positive and negative peaks are proportional to the charge on the particle. The typical detection limit of an image charge detector is several hundred charges.[17]

2.4 Results and Discussion

Several methods could be used to improve the planar EIBT performance. Achieving good resolution with image charge detection may need to be developed. First, the copper target plate could be biased at a high voltage: 2500 V ~ 4000 V. Time-lag

focusing could be applied between ionization and extraction of the ions out of the ion source into the EIBT. Ions could be extracted from the source by an electric voltage on the target. The effect of the time delay and the extraction voltage could be optimized to achieve good resolution. The same kinetic energies with copper ions were produced after they passed the grid, which is grounded. Second, three cylinders as an Einzel lens could be set up between the ion source and the planar EIBT. This would focus more ions to enter the planar EIBT if there was a larger ionization surface. Third, the surface of the copper plate could be cleaned by methanol three times. The sandpaper could polish the copper plate surface smoother. It is important to not contaminate the plate. Finally, I could try other metal samples such as Ag or Pb to see whether the N_2 laser energy on the sample plate would be enough to ionize these metal materials.

There is another important consideration involving the injection angles of the ions. Based on the SIMION 7 calculations, the injected angles of the ions are critical, and are related to the ions' energy. If the kinetic energy of the copper ions is between 3.1 keV to 4.5 keV, the azimuthal injection angle should be less than one degree ($-1^o \leqslant \alpha \leqslant 1^o$). When the kinetic energy is from 3.1 keV to 4.5 keV, the elevation injection angle must be less than six degrees. ($-6^o \leqslant \varepsilon \leqslant 6^o$). In these ranges, the injected ions could be well trapped in the EIBT. As we mentioned, the kinetic energy of the trapped ions is also related to the potentials on the ion mirrors. If the ions' kinetic energy is larger than the potential energy on the ion mirrors, the ions will pass through the trap. If the ions kinetic energy is small, ions could not pass the potential field from the Einzel lens.

As ions leave the EIBT, they could be detected by the microchannel plate detector (MCP). The MCP signal is then amplified and recorded. The signals from the MCP verify

the alignment between the ion source and the EIBT. The MCP is suitable for a flight instrument such as is used in time-of-flight mass spectrometry and multiple-reflectron mass spectrometry. It multiplies the detection of the electrons or ions and also provides spatial resolution based on its many separate channels.[26]

The instrument sensitivity is dependent on the number of ions produced from the copper sample plate and the number of ions detected by the image charge detector. Increasing the number of ions produced can be achieved using another ionization method or instrument for sample. The factors affecting ion detection include the transmission of the grid in front of the sample plate, truncation of the ion beam with potentials at the entrance of the ion mirror, and the ion focusing ability of the EIBT. The EIBT sensitivity is limited by the dynamic range, which is limited by the image charge detector and electronics and the signals produced from trapped ions. Various particle sizes and impact velocities also affect the instrument sensitivity.

The number of ion cycles is related to the resolution of the EIBT. It depends on the vacuum conditions in the chamber because of ion collusions with residual gas molecules. The pressure determines the mean free path of the ions, therefore affecting the performance of the mass analyzer. The mean free path for metal ions in the EIBT is given as

$$\ell = \frac{k_{\mathrm{B}}T}{\sqrt{2}\pi d^2 p} \qquad (1)$$

where k_{B} is the Boltzmann constant, T is temperature, p is pressure, and d is the diameter of the particles.

Suppose the mean free path of the ions of various weights (A, B, C, D and E) in different pressures (10^{-6} torr, 10^{-7} torr and 10^{-8} torr) are calculated by the above equation. (Table 1)

The diameter of A is 0.04059 nm,[27] The diameter of the B is 0.18 nm, The diameter of the C is 0.288 nm, The diameter of the D has around 1 nm/particle.

Table 1. Estimated mean free path for molecules A, B, C, and D

	Weight (g/mol)	Mean Free Path Length (m)		
		10^{-6} torr	10^{-7} torr	10^{-8} torr
A(H)	1	435.2	4352	45320
B(B)	10	214.9	2149	21490
C(Ag)	108	83.95	839.5	8395
D(Peptide Bradykinin)	1060	6.96	69.6	696

After we calculated the mean free path for various molecules, the number of (2)
cycles is equal to the mean free path divided by one cycle length of molecules. Suppose the cycle length is 20 cm for these particles. The number of cycles for A, B, C, D and E in 10^{-7} torr are 21760, 10745, 4197 and 348. Based on these calculations, we found that the EIBT design was suitable for large molecule analysis because it has good resolution for large molecular weight molecules. The following equations can be used to calculate the resolution of various molecules: A, B, C, D and E. The number of cycles is proportional to the velocity of the ion. Therefore, $V_1/ V_2 = n_1/n_2$ n_1- the number of cycles for m_1; n_2- the number of cycles for m_2

The kinetic energy of various mass to charge (*m/z*) ions should be the same because of the sample plate with one high voltage. It could be presented in the equation 3.

$$½ m_1V_1^2 = ½ m_2V_2^2 \quad (3)$$

The peak separation Δm which distinguish two ion peaks m_2 and m_1 is the resolution of mass spectrometer.

$$\Delta m = m_2 - m_1 \quad (4)$$

The resolving power R is defined as

$$R = m/\Delta m \quad (5)$$

Supposing the number of cycles for m_1 (108 g/mol) is 4198 and the number of cycles for m_2 (109 g/mol) is 4197, the resolution should be around 2100 from the above equations. The resolution of different ions is related to the number of cycles for the analysis. As in our case, large ions should have more cycles in the EIBT. The EIBT can readily reach high mass resolving power (> 10^5) in 10^{-8} torr. Therefore, the miniaturized EIBT has a higher resolution than Zajfman's design which needs 10^{-10} torr to achieve 10^5 resolving power. The estimated mass resolutions for various molecules are presented. (Figure 23)

Table 2 Variuous molecules' (A, B, C, D) estimated mass resolutions in planar EIBT

	weight(g/mol)	Mass resolution m/Δm		
		10^{-6} torr	10^{-7} torr	10^{-8} torr
A	1	2176	21760	217600
B	10	1074.5	10745	107450
C	108	420	4200	42000
D	1060	34.8	348	3480

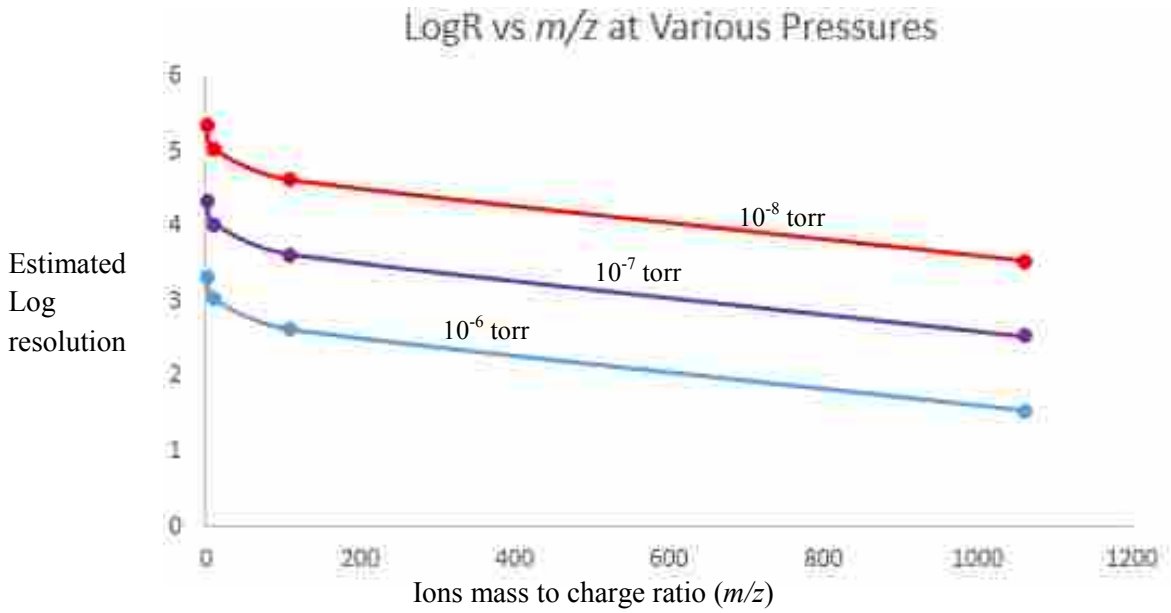

Figure 23. The relationship between particle weight and mass resolution is presented in the planar EIBT. The resolution decreases with the particle weight increasing in my EIBT. Ultra-high vacuum conditions are better for mass resolution.

We compared the ion entry angles between the Zajfman design and our planar EIBT in SIMION when the ions have the same kinetic energy, 4 keV. (Figure 24 a & b) The Az (Azimuth) and EL (Elevation) entry angles functions in SIMION could display the starting flight direction of the selected ions. When the ions enter the trapping region in these angle ranges, they could be trapped in EIBT. The Az entry angle range in our planar EIBT is $-1.1^\circ \leq Az \leq 1.1^\circ$ and the EL entry angle in our planar EIBT is $-1.5^\circ \leq EL \leq 1.5^\circ$. These are larger than the Az ($-1^\circ \leq Az \leq 1^\circ$) and EL ($-1.1^\circ \leq EL \leq 1.1^\circ$) in Zajfman design. The larger range of the entry angles indicated there were more ions trapped in the planar EIBT. This could increase the sensitivity of the mass analyzer. Because more ions were trapped in this small device, the space charge issue could not be ignored. The space

charge could be modeled by selecting “Ion Beam” type under the Repulsion panel in SIMION. Each ion repels or attracts other ions when they fly back and forth in the EIBT. This does not seem have a dramatic difference between the planar EIBT and the Zajfman EIBT when a large number of ions enter the trapping region. Many other parameters also could affect the ions' motion. The geometry of the electrodes and the potential gradients on the ion mirrors were optimized by SIMION. The focusing potential on the Einzel lens could control the shape of the ion beam. The space charging between two planar plates in our EIBT may also change the number of trapped ions. The optimized space between the two plates is around 1 cm after SIMION simulation. The Einzel lens potential in Figure 2.16 was 3500 V. The highest potential on an electrode in the ion mirror was 5000 V. The kinetic energy of the ions was 4 keV. The trapped ions' *m/z* was 100. The x axis represents the ions' azimuthal ejection angle and the longitudinal coordinate is the elevation injection angle.

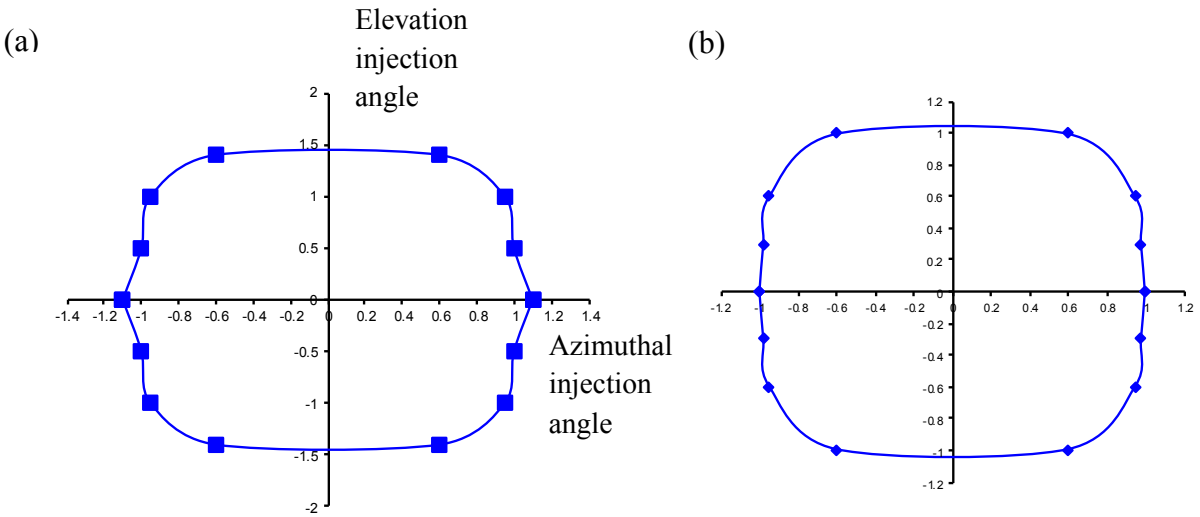

Figure 24. The entry angle ranges in EIBT. (a) Our planar plate EIBT region; (b) Zajfman's EIBT trapping region

Although the planar plate EIBT did not produce signals from the image charge detector, we estimated the resolution for various molecules. The performance of the planar EIBT could be better than Zajfman's EIBT basing on smaller size and cycle length. Zajfman's EIBT resolution at 10^{-8} Torr is 200~300 for *m/z* 100 ions but our planar EIBT resolution is 1000~1100. We thought that the only difference between the planar EIBT and Zajfman's EIBT should be the electric field in the YZ view. Zajfman's EIBT has a round shape electric field which is probably better for trapping more ions as they pass through the field free region. Our planar EIBT probably did not trap enough ions to generate signal in the image charge detector. After that, we developed another new type of EIBT which is made using Kapton film. The film can be rolled into one column to provide a round shaped electric field. When the ions are injected into the column, they could be better trapped.

Chapter 3 Miniaturized Electrostatic Ion Beam Trap Made From Rolled Kapton Film

3.1 Introduction

Another new electrostatic ion beam trap was set up in our lab. It was made from Kapton film, a flexible material which was previously used to design a flexible circuitboard reflectron.[28] The new flexible miniaturized electrostatic ion beam trap (EIBT) mass analyzer is small (4.5 cm × 8 cm), light weight (~ 1 g) and showed better resolution than the previous EIBT design (Figure 25). The previous EIBT size was 28 cm × 10 cm which is significantly bigger than the flexible EIBT. The number of cycles in the flexible EIBT may be more than in the planar EIBT due to the small size. There are seven thin copper with tin overlay traces (10 mm wide by 0.05 mm thick) deposited onto each side of a flat, flexible circuit board polyimide (Kapton) film. The space between adjacent traces is 1 mm. Three wide traces comprise an Einzel lens (5 mm wide by 0.05 mm thick) on each side and are close to the center of the Kapton film. The space between the two wide traces is 0.5 mm. A voltage gradient is formed from these tin rings.

We can change the traces' thickness, size and spacing during the deposition process. This feature could help us to obtain more precise voltage gradients. The circuit board substrate was rolled to form a cylindrical shape. One Teflon tube (OD 1.4 cm) approximately 0.2 cm thick, supported the flexible Kapton film roll with the film roll held inside the Teflon tube. The Telfon tube has a slight opening through which one end of the Kapton film can extend. The voltage mirror in the mass analyzer consists of seven electrodes with various voltages. The electrodes' voltages were 0 V, 1000 V, 2000 V, 3000 V, 4000 V, 5000 V and 0 V. The potentials on the three wide Einzel lens electrodes were 0 V, 3500 V and 0 V. A metal cylinder was located at the center of the flexible

EIBT. It was connected to a charge sensitive preamplifier (Amptek A250) and three amplifiers (A275). The ion frequency signals were collected by an oscilloscope, and mass analysis was obtained by Fourier transform.

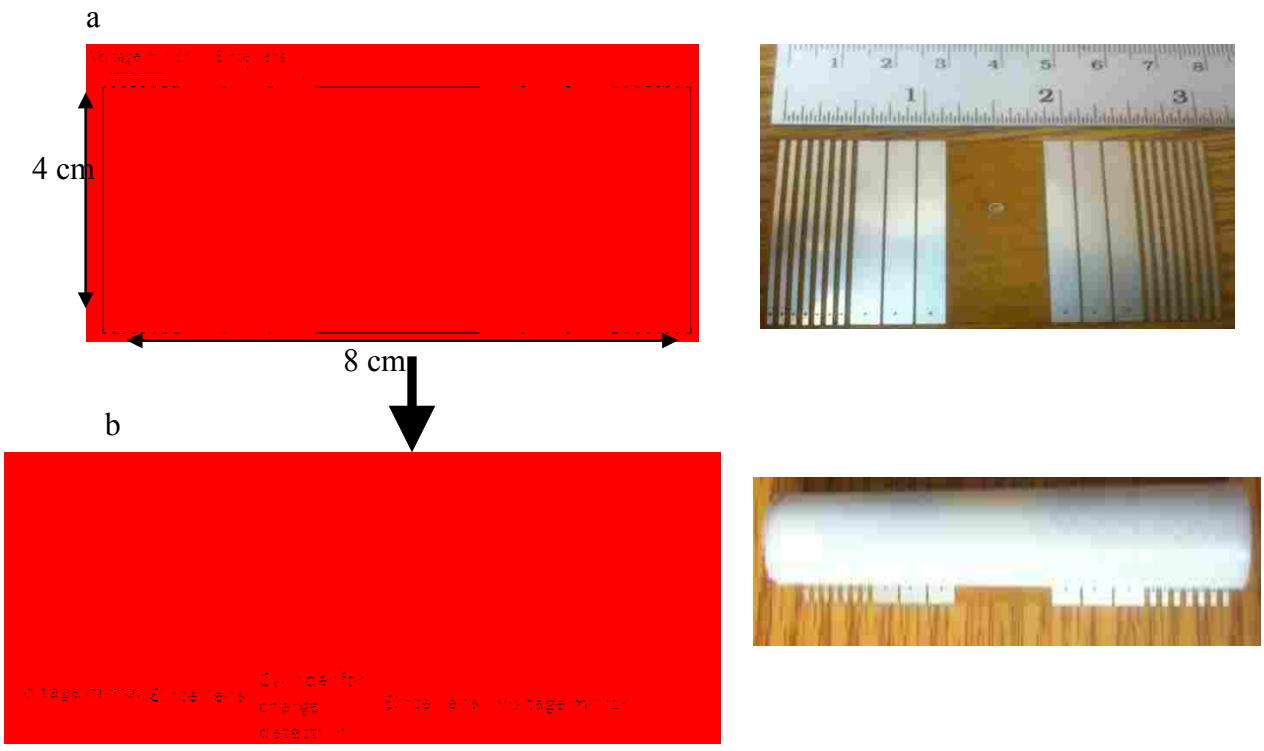

Figure 25. (a) The schematic diagram of our flexible electrostatic ion beam trap. There are seven thin tin traces on each side. The voltages are 0 V, 1000 V, 2000 V, 3000 V, 4000 V, 5000 V and 0 V. The Einzel lens consists of three wide traces whose potentials are 0 V, 3500 V and 0 V. (b) A schematic diagram of the rolled electrostatic ion beam trap.

3.2 Simulation of the Flexible EIBT

The electrical field in the flexible EIBT is the same as the electrical field in Zajfman's EIBT. The Kapton film column design also generated a round shape electrical field in the YZ view. The 3D view of the flexible EIBT was produced using SIMION 7 (Figure 26). There are two electrostatic mirrors on both sides of the flexible EIBT.

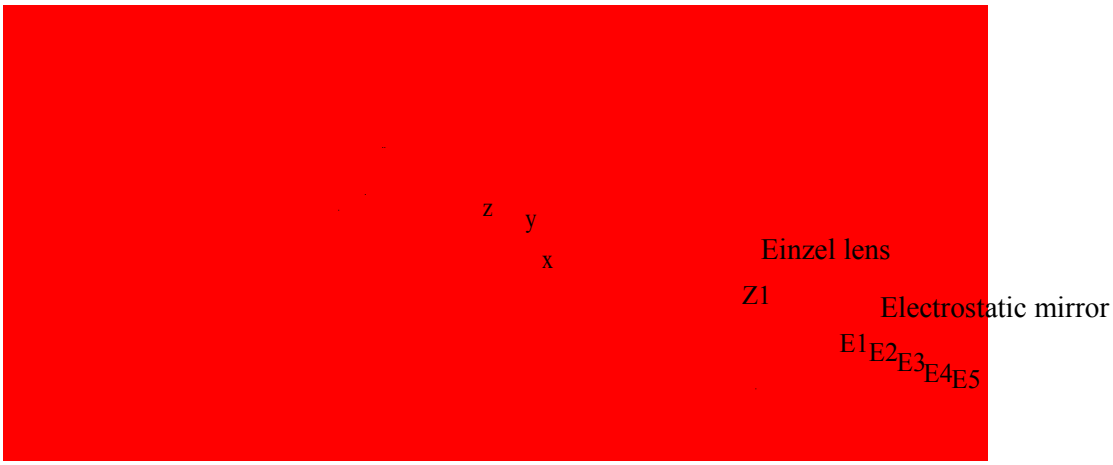

Figure 26. Three-dimensional view of the flexible EIBT in SIMION 7. The electrostatic ion mirror had potential of E1 = 1000 V, E2 = 2000 V, E3 = 3000 V, E4 = 4000 V and E5 = 5000 V. The Einzel lens consists of A1, Z1 and Z2. The voltage on Z1 is 3500 V. A1 and Z2 are grounded.

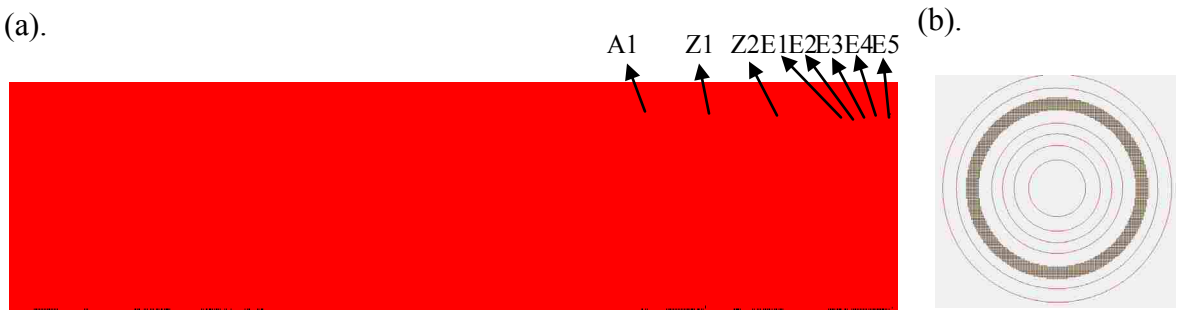

Figure 27. (a). The electric field of the flexible EIBT in XZ view. (b). The electric field of the flexible EIBT in YZ view. The electric field in the flexible EIBT was the same as the electric field in the Zajfman's EIBT.

Based on a SIMION 7 simulation, the electric field (XZ view or YZ view) of the flexible EIBT is the same as that of Zajfamn's EIBT.[19] The potential function in the Y dimension is presented from SIMION. The ring electrodes in the flexible EIBT should provide the same potential function in the Y or Z dimension.

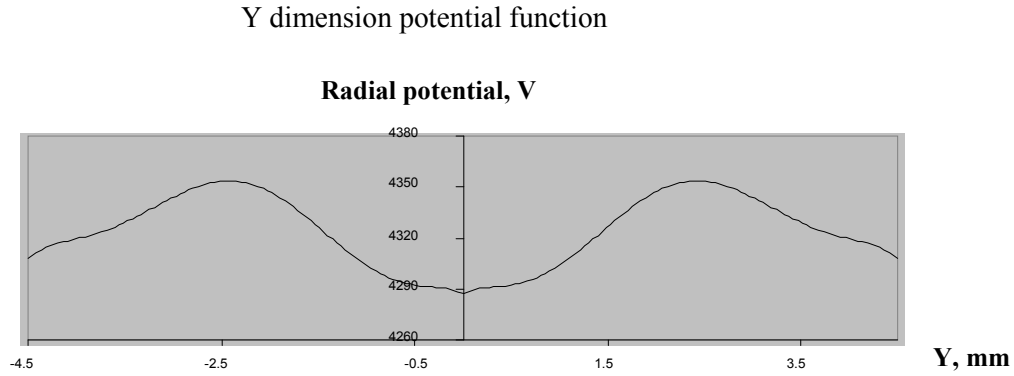

Figure 28. The potential function of the flexible EIBT in the Y dimension.

The ion motions in the trapping regions should be very similar. Space charge during the ion reflecting period has obvious affects in our miniaturized mass analyzer device.[29-30] However, our design was smaller than Zajfman's EIBT which contributed to more ion cycles in the flexible EIBT. This is better for resolution performance. The sensitivity of the flexible EIBT should be similar to the Zajfman's design.

3.3 Design of Flexile EIBT & Experimental Set-up

3.3.1 Flexible EIBT Electrodes Made by Conductive Silver Pen

We tried to make electrodes on the EIBT by ourselves using a conductive ink silver pen. This pen, filled with a conductive ink, was previously used to fix broken electrical lines on a printed circuit board. Researchers at the University of Illinois at Urbana-Champaign have demonstrated electronic circuits on paper.[31-32] To do this, a line was drawn and after it dries, the silver line can conduct electricity. They used it to build a LED display with a five-volt battery. However, we realized it is too difficult to make metal electrodes on Kapton film. The Kapton film surface was too smooth. Therefore, the metal electrode thickness and shape on the Kapton film were difficult to control. There were always some gaps on the electrodes I drew. When high voltages were applied to these electrodes, the required electric field could not be set up. After that, we decided to deposit tin electrodes on the Kapton film.

3.3.2 Tin Traces Deposited on Kapton Film as Electrodes

The tin traces were deposited on the Kapton film by Flexible Circuit Tecnologies. They were 0.05 mm thick. The electrodes on the ion mirrors were 1 mm wide and the distance between two electrodes was 1 mm also. The Einzel lens electrodes are 0.5 cm

wide and the distance between two of the electrodes is 0.5 mm (Figure 29a). The voltages on the flexible EIBT electrodes were applied with the same sequence as those on the planar EIBT.

The electrode positions on the flexible EIBT were optimized to produce the desired electric field. The maximum potential on the ion mirror is 5000 V. The other electrode positions of the ion mirror were placed following the equipotential lines generated by the electric field from the 5000 V electrode. Thus, we were able to set up the ideal flexible EIBT. We compared the potential valley between the flexible EIBT and Zajfman EIBT using SIMION.

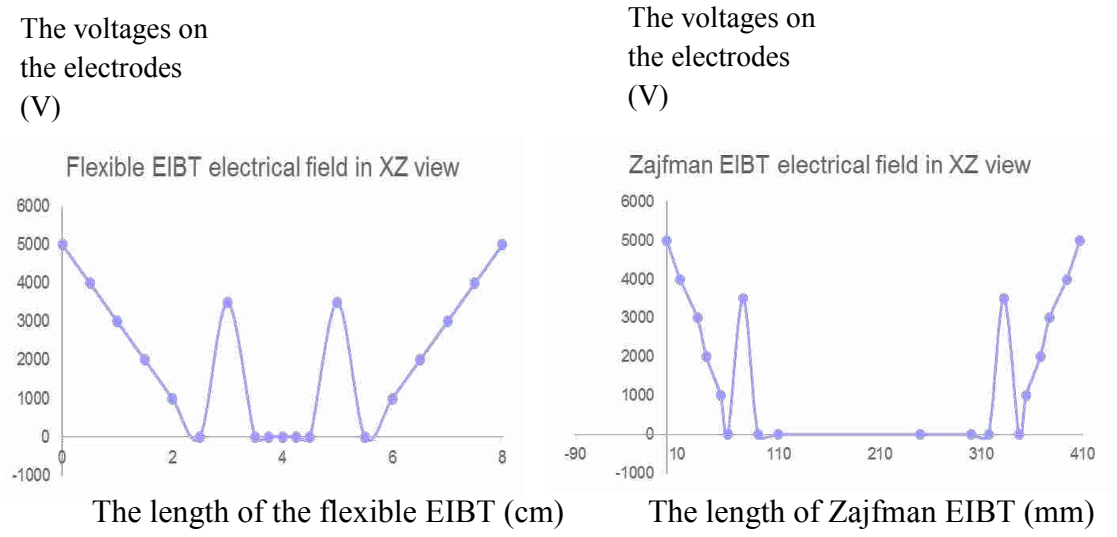

Figure 29. The electrical fields of the flexible EIBT (left) and the Zajfman EIBT in X-Z view. The X-axis represents the length of the ion trap and the Y-axis represents the potentials on each electrodes. Our flexible EIBT potential drops were smoother than those of Zajfman EIBT.

3.4 Experiment Setup for the Flexible EIBT

A cesium iodide sample was used to test the flexible EIBT. 0.5 g cesium iodide was dissolved in 2 mL of water-methanol (90%-10%). The solution was spread out on a copper plate. After 12 hours, the cesium iodide recrystallized on the copper surface. A pulsed nitrogen laser at a wavelength of 337.1 nm (model NL100, Stanford Research) with a pulsewidth of 4 ns was used to ionize the sample. The output energy of the laser was 170 μJ. One bi-convex lens with a focal length of 7.5 cm was used to focus the laser beam onto the CsI sample.

A charge detector was also used to obtain the frequency of the ions in the flexible EIBT mass analyzer. The charge sensitive preamplifier is an Amptek (Bedford, MA) A250 on a PC250 circuit board, and three Amptek A275 amplifiers on one PC275 circuit board. The charge detector consisted of one cylinder in the field-free region of the ion trap. The cylinder was connected to the preamplifier and amplifier which were shielded by a copper box.[33]

At the end of the EIBT, a microchannel plate detector was set up. There were two functions for the microchannel plate detector (MCP). First, it could detect the neutrals produced by ion collisions in the trapping region. It was very important to us to measure the lifetime of these ions. Second, it was used to check the alignment. The MCP was designed to handle the fast ion pulses typical with time-of-flight MS. It has a 50 ohm output and sub-nanosecond rise time. There are three microchannel plates aligned in a Z shape. Various potentials -2900 V, -2200 V, -1500 V, and -800 V were applied to each plate. (Figure 30) The anode in the MCP will receive the electrons and transfer the signals to the oscilloscope.

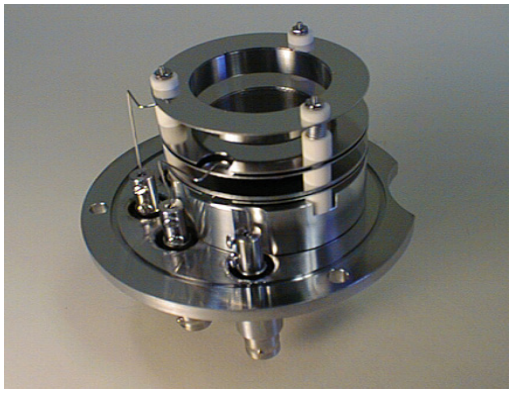

Figure 30. This 25 mm microchannel plate detector was used for ion detection. (Jordan TOF products, Inc.)

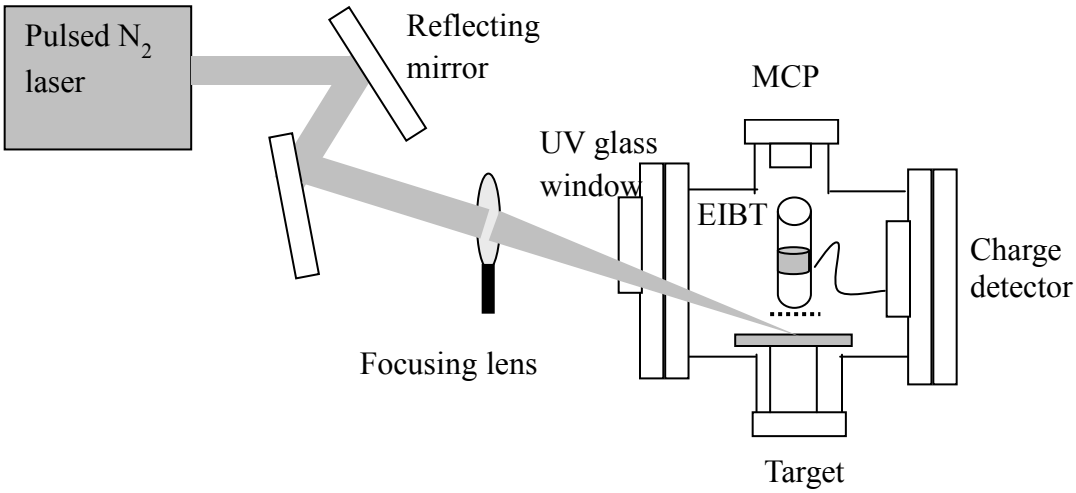

Figure 31. The flexible EIBT experimental setup. The microchannel plate detector was used for alignment. The charge detector measured the frequency of the ions passing the field free region.

The flexible EIBT experimental setup was similar to the planar EIBT experimental setup (Figure 31). A Stanford Research Systems NL100 nitrogen laser was used to ionize the sample which was then subjected to high voltages. A high ion transmission grid was in front of the sample. The grid was grounded. The ions were accelerated to the desired kinetic energy usng the resulting electric field. The ion flight time from the Cs^+ sample plate to the flexible EIBT was around 1 μs based on theoretical calculations. Each cycle time of Cs^+ in the flexible EIBT was around 3 μs based on a SIMION simulation calculation. Then, the Stanford Research Systems DG535 pulse/delay generator (risetime of 5 ns) triggered the DEI PVX-4110 high voltage pulse generator (risetime of 10 ns) 2 μs after the laser pulse. The high voltages could be switched on and off at the entrance electrostatic mirror. A potential valley could be set up in the EIBT. After 15 ms, the entrance electrostatic mirror potentials were switched off to release the ions from the EIBT. The same procedure was repeated and the CsI ion signals were detected by the image charge detector. (Figure 3.8)

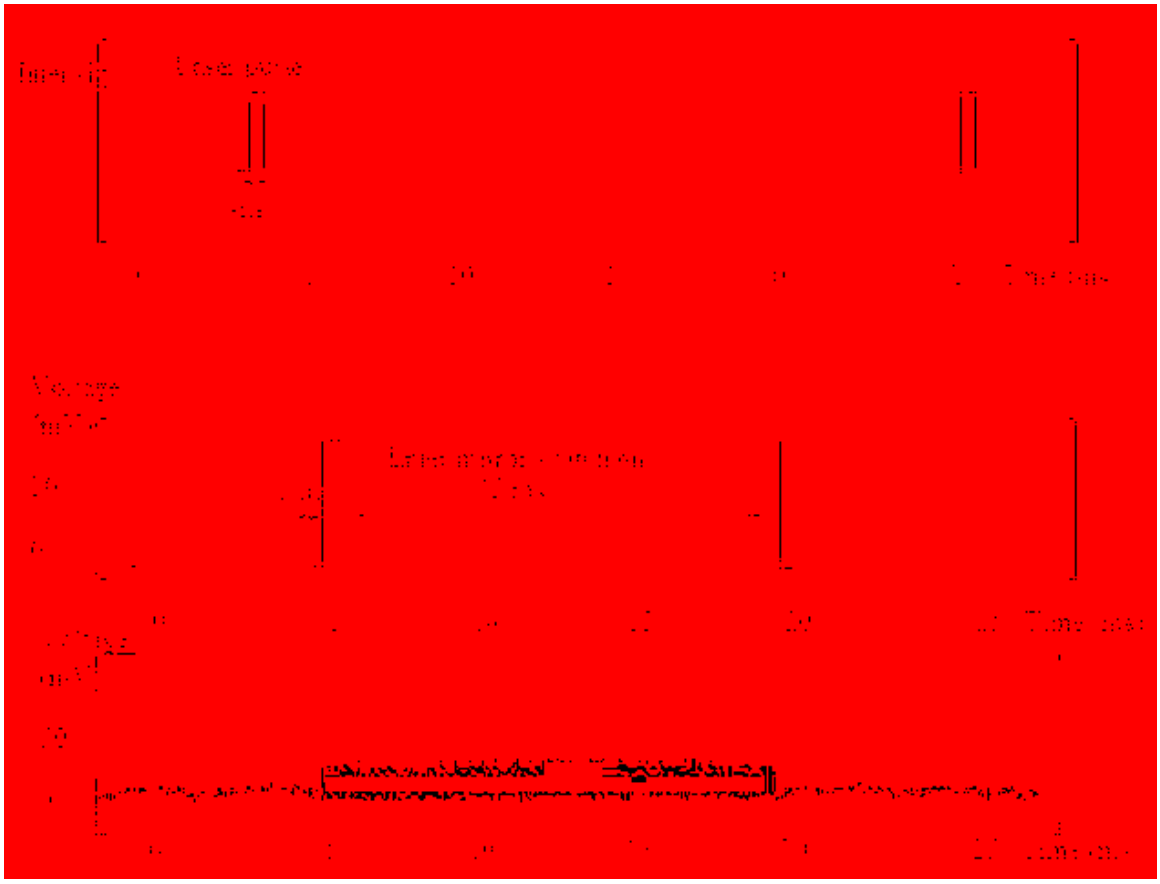

Figure 32. (a).The flexible EIBT experimental pulse sequence. The laser pulse was 4 ns in duration and the laser frequency was 25 Hz. (b). After 2 μs, the high voltages were applied to the entrance mirror electrodes. The ions were trapped in the EIBT. At the conclusion of the experiment, the entrance electrodes were switched off after 15 ms. (c) The CsI signals detected by the charge detector during the period of 15 ms (2296 cycles). The trapping period depended on the laser pulse frequency.

3.5 Results and Discussion

The cesium iodide (CsI) was ionized by the nitrogen laser and the CsI ions were first detected by the microchannel plate. This demonstrated that the ion production and alignment were good. When we changed the voltages on the sample plate, peaks did not appear. This confirmed that the signals were from the sample plate, not from noise. The CsI signals from the MCP are presented in Figure 3.9. The Cs^+ ions traveled in 3.18 μs to the MCP while the simulation time from SIMION 7 was around 3.20 μs. The Cs_2^+ ions traveled 4.48 μs to the MCP and the theoretical time was 4.52 μs. The Cs_2I^+ ions traveled 5.49 μs and the simulation time was 5.50 μs. Therefore, the most abundant peak was from Cs^+; the Cs_2^+ peak is less abundant; and the Cs_2I^+ peak is the least abundant. The CsI mass spectrum from the MCP is presented in Figure 34.

Table 3. The theoretical arrival time and actual time of Cs+, Cs2+ and Cs2I+ based on MCP signals.

Ions	Exact Mass（amu）	Theoretical arrival time from SIMION (μs)	Actual arrival time from MCP spectrum (μs)
Cs^+	132.91	3.20	3.18
Cs_2^+	265.81	4.52	4.48
Cs_2I^+	392.71	5.50	5.49
$Cs_3I_2^+$	652.51	7.06	7.01

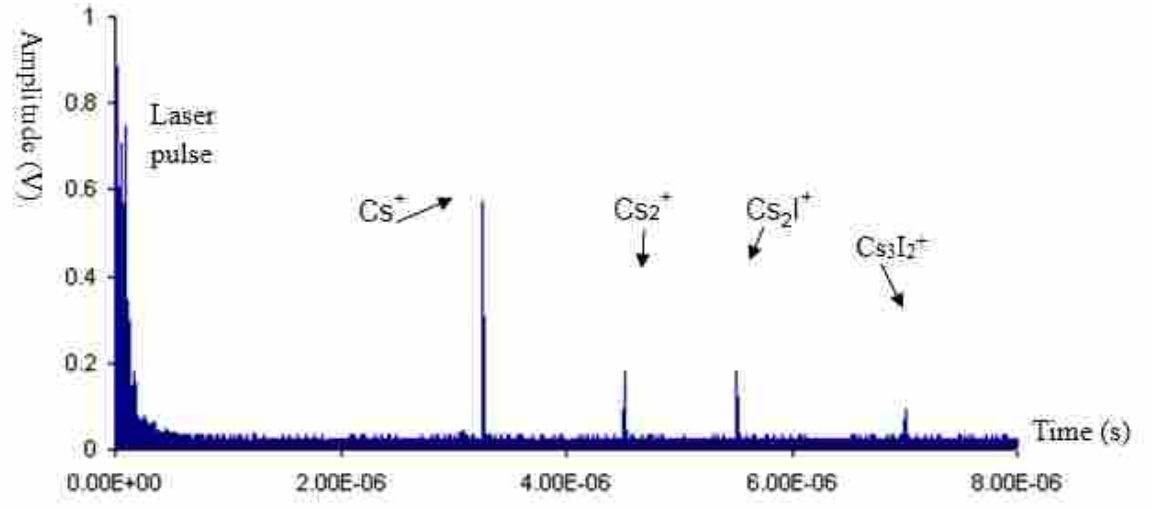

Figure 33. The MCP signal obtained with the flexible EIBT turned off. When the potential on the sample plate was decreased, the arrival times of the ions were longer. The ion peaks moved when the sample plate voltages changed.

The mean free path of Cs^+ is around 247.9 m at 10^{-7} Torr. The estimated cycle length from SIMION is around 12 cm. The number of Cs^+ ion cycles is around 20670. The estimated trapping time is around 40 ms when the sample plate voltage is 2500 V.(Figure 33) The measured flight times from the MCP were slightly different from the calculations made with SIMION. One contributing factor was the imperfections in the flexible EIBT. Even using the flexible EIBT rolled in a Teflon tube, the electrodes on the film were different from the ring electrodes. Another factor was the ions were leaving the sample plate at a single angle in the simulation. They have some distribution of kinetic energies and various dispersive angles, which lead to deviations from the calculations made with SIMION.

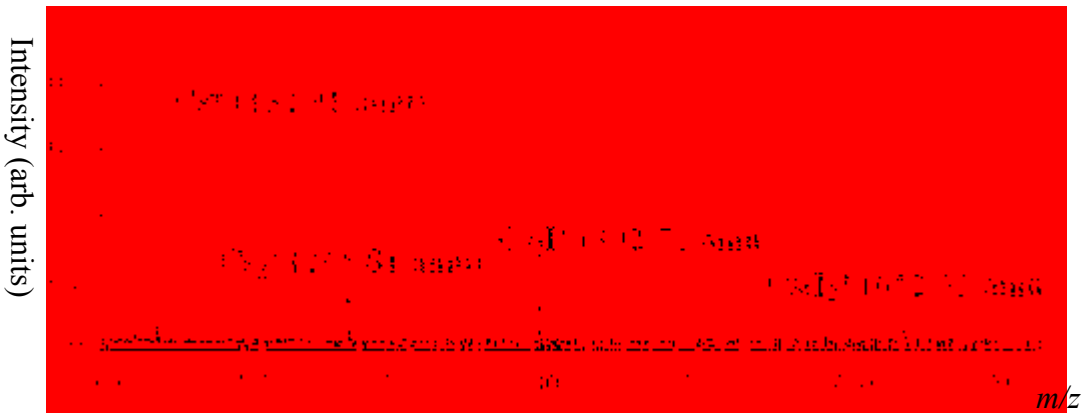

Figure 34. The CsI mass spectrum from MCP obtained using the flexible EIBT.

The flexible EIBT also used an image charge detector. The numbers of CsI ion cycles were recorded by the image charge detector. The frequency domain spectrum of CsI is presented in Figure 3.11. The data were sent to an oscilloscope and use Matlab to convert the data to the frequency domain spectrum using the Fourier transform function. The mass spectrum of CsI is presented in Figure 3.12. We also could determine how many charges were trapped based on the peak area generated by the image charge detector. The resolution for the Cs^+ ion was ~1000 and the resolution of the Cs_2I^+ was around ~1700 based on the equation $R = f/2\Delta f$.

Our design did not perform as well as Zajfman's EIBT. The first reason was that our miniaturized device operated up to 10^{-7} Torr but they worked at 10^{-10} Torr for their device. The mean free path of the ions in our device was obviously shorter than theirs. Therefore, our flexible EIBT resolving power could not achieve 10^5 as they did. Next, space charge was a large factor in our flexible EIBT. The ions repelled each other at the turning point.

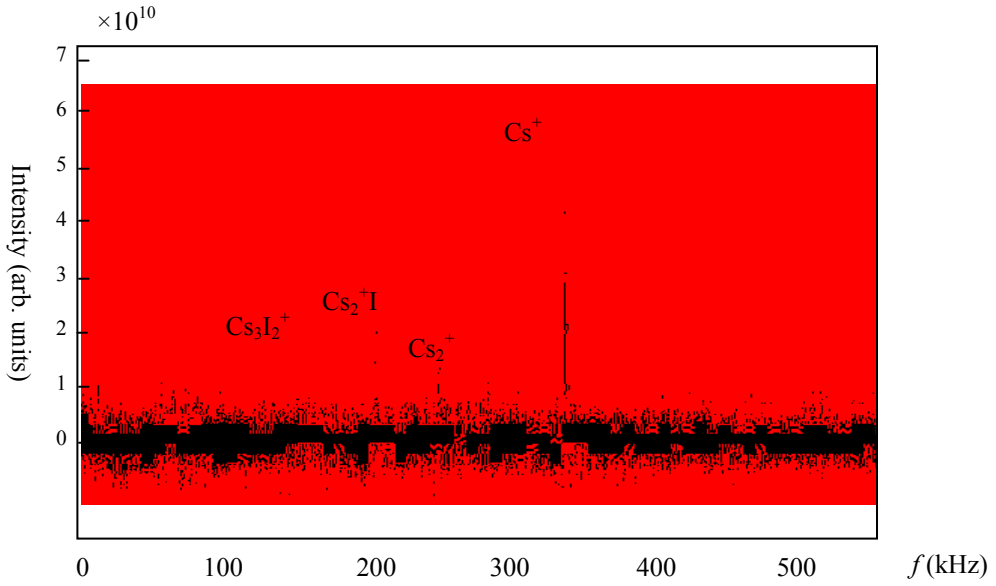

Figure 35. The frequency domain spectrum of CsI after Fourier transforms. The Cs+ ion has a frequency of 325 kHz and the first harmonic can be seen at 650 kHz.

Last, the number of ions entering the trapping region of the flexible EIBT was smaller than the number of ions entering their linear EIBT. This resulted in a smaller S/N ratio. Even though the miniaturized flexible EIBT had some disadvantages, it is still a good resolution instrument compared to other miniaturized ion traps. The mass accuracy of Cs^+ is better than 0.1%. The difference of Cs^+ exact mass and measured mass Δm is divided by the exact mass of Cs^+. (Figure 36) This could be used for applications in the fields of outer space exploration, medical analysis and safety examination.

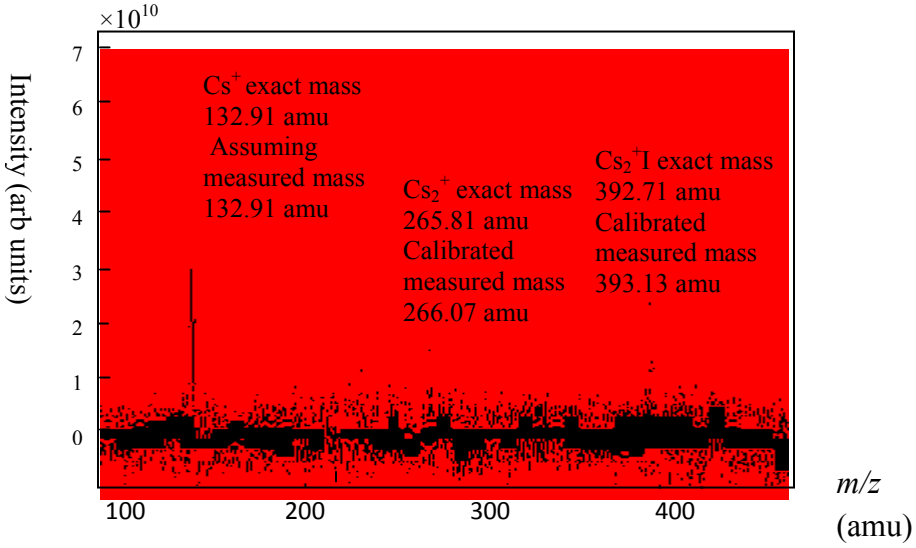

Figure 36. The mass spectrum of CsI after Fourier transform The Cs+ ion has exact mass 132.91 amu which was used for calibrating other ions to check mass accuracy. The mass accuracy of Cs2I+ is less than 0.1 %.

The trapping time of CsI in the flexible EIBT was up to 200 ms. The CsI ions' signals were decayed in the system because of colliding with residual gas. (Figure 37)

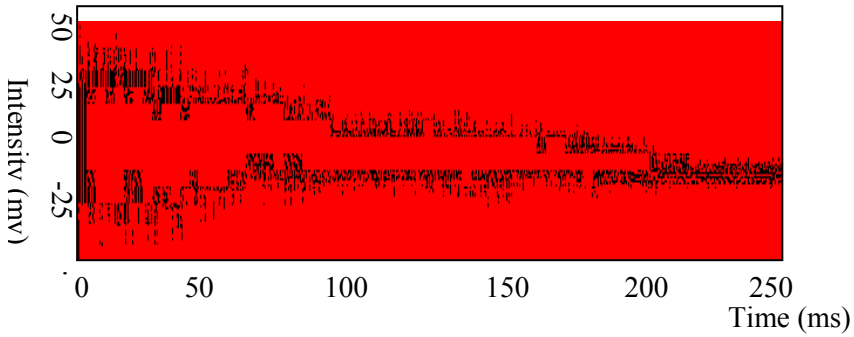

Figure 37. The trapping time of the CsI in the flexible EIBT was around 200 ms.

The higher harmonics should be detected for this long observation time. It indicates a better mass resolution result of CsI is coming with this flexible EIBT. (Figure 38) . Longer detection time means more cycles in the flexible EIBT which result in better resolution performance. The oscillations of the ions are not affected by trigger jitter, response time the MCP, etc.

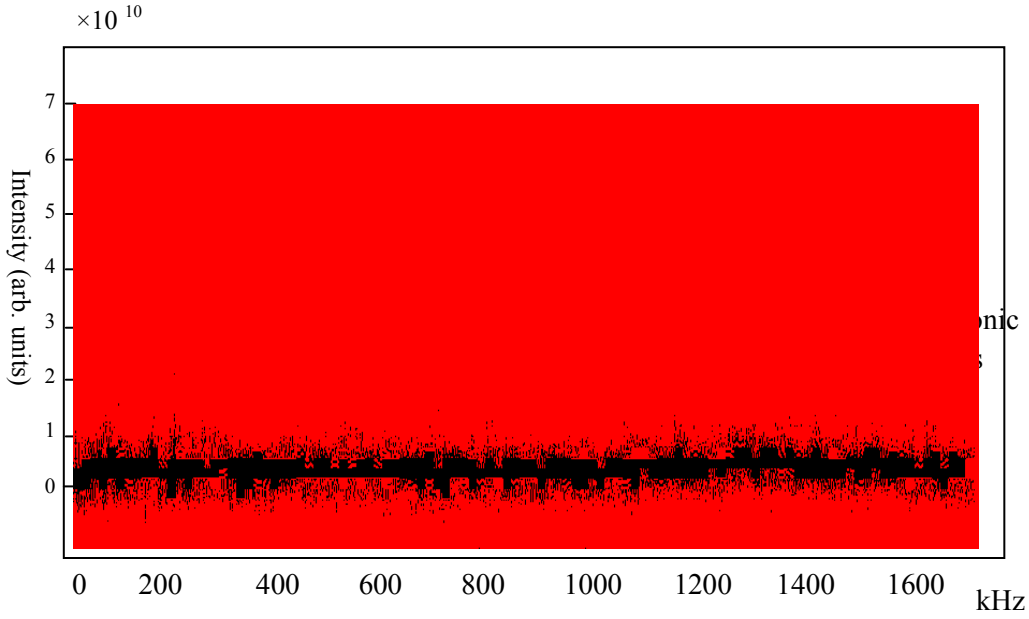

Figure 38. The frequency spectrum of CsI is from the number of cycles in the decay time. The 3rd and 5th harmonics of trapped Cs+ ions are showing. The mass resolution of Cs+ is calculated as $R = m/\Delta m \approx 11600$ basing on the 5th harmonic.

Chapter 4 Future Work and Conclusions

4.1 Future Work

Several methods could be used to improve the performance of the flexible EIBT. First, we could set up a multiple-stage image charge detector on the Kapton film. Brandon Barney in our group has successfully detected highly-charged polystyrene ion signals using a multiple-stage image charge detector which consisted of two printed circuit boards. A multiple-stage image charge detector could increase the S/N ratio as proved by Qi Sun.[34] They introduced a dual-cylinder image current detector in an EIBT and it improved the detected signal (S/N) strength more than ten times comparing to the single cylinder detector in an EIBT. We could design a two-stage image charge detector on Kapton film to improve the S/N. The design is simple to align and a less expensive way to improve the EIBT performance.

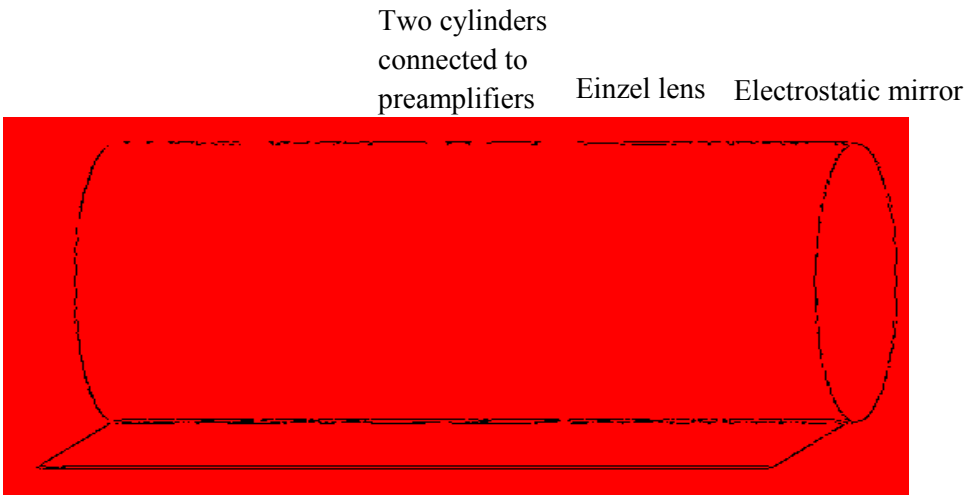

Figure 39. The new flexible EIBT with two cylinder image charge detectors.

Next, an Einzel lens system could be set up between the sample plate and the flexible EIBT. It would help to focus more ions as they enter the trap. The flexible EIBT S/N performance may be improved. The Einzel lens could also work as a new type of pulse chopper for mass selection.[35] When the voltage on the Einzel lens middle electrode increased from 8 kV to 14 kV, all the ions are reflected upstream based on SIMION simulations.(Figure 40) The voltage timing on the Einzel lens would be controlled by a pulse/delay generator.

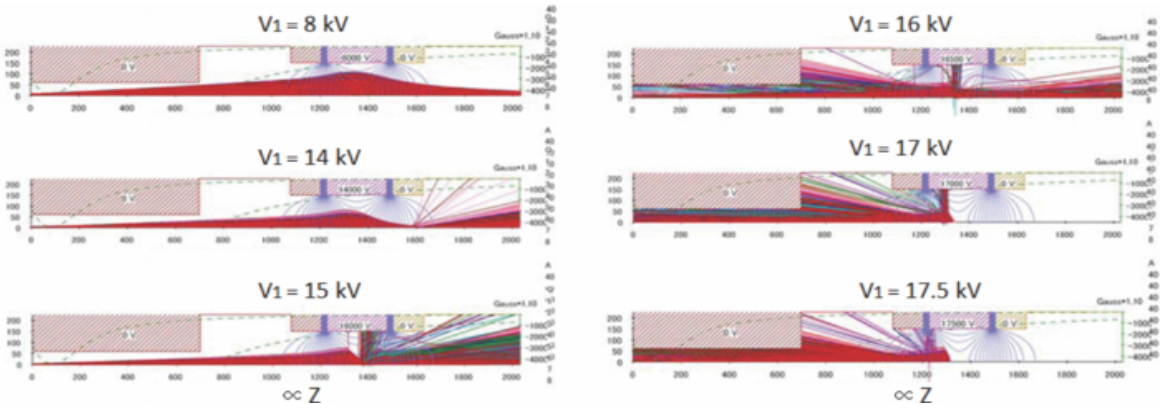

Figure 40. Simulated tracks of ions from the cathode to the anode and from the anode through the Einzel lens, where V1 = 8–17.5 kV. The blue line represents the electric field and the red line is the ion bunch.[35]

Third, the miniaturized flexible EIBT could be modified as an array of ion trap mass analyzers. The new mass analyzer array with multiple ion trapping and analyzing channels should have a performance similar to multiple ion trap mass analyzers. It could have multiple ion storage space and perform mass analysis simultaneously. The

sensitivity of an array of flexible EIBTs should be better than the sensitivity of a simple flexible EIBT (Figure 41).

Figure 41. Four flexible electrostatic ion traps in parallel set up as an array of flexible EIBTs.

Fourth, the lifetime measurement of biomolecules was analyzed using an electrostatic storage ring with electrospray ionization in the Andersen research group.[36] They stored a sufficient number of ions to study the decay of metastable ions and to determine destruction cross sections. The number of ions in a bunch was estimated at around 10^3~10^4 assuming the decay time was around 0.1 s. Therefore, our flexible miniaturized EIBT could be applied to the analysis of the lifetime of bovine insulin (*m/z* 5734) and the peptide bradykinin (*m/z* 1060).[37] An electron collision study of the biomolecules could also be undertaken. The cross section and trapping cycle could be measured. The external electrons were produced by electron gun.

Finally, the miniaturized flexible EIBT mass analyzer could be used to build a portable mass spectrometer for medical analysis. An atmospheric pressure ionization method such as ESI or atmospheric pressure chemical ionization should be employed

with the portable mass spectrometer (MS). Ambient ionization methods such as desorption electrospray ionization (DESI) and low-temperature plasma (LTP) have already been successfully tested in the Mini^{TM} handheld mass spectrometer by the Ouyang research group.[38] A portable turbomolecular vacuum pump was used for the miniaturized mass spectrometer.[39] The miniaturized mass spectrometer is convenient for in-situ analysis. It is more accurate than traditional mass analysis in lab to achieve the ions mass-to-charge ratios (*m/z*). As we know, the sample could be changed such as preconcentration or derivative by itself during the delivery. The portable MS helps achieve the goal that the lab is taken to the sample, not the sample to the lab. It is simple to operate by end users, affordable, and lower power.

Our planar EIBT was not successful in capturing the ion signals. However, Dr. Austin *et al.* at BYU have already demonstrated two dimensional planar plates that are suitable for trapping ions as well as those 3-D ion trap mass analyzers.[40-42] A planar plate ion trap could have the same electric field as a 3-D mass analyzer. Therefore, the two printed circuited board EIBT should be tested again in future work.

4.2 Conclusions

After the W. Brinckerhoff research group used flexible Kapton film as circuitboard material to construct a reflectron in 2000,[28] we were able to take advantage of this new technology to design a new miniaturized flexible EIBT. The new flexible EIBT is inexpensive ($200/each), small (8 cm × 4.5 cm), light weight (less than 1 gram), and easy to couple with various ionization methods. The resolution is better than what is typical for traditional miniaturized mass analyzers. There is no mass limitation for EIBT analysis.

The flexible EIBT setup was successfully tested with laser ionization using a CsI coated impact plate. Simulations of the flexible mass analyzer with a tilted impact plate show that product ions from laser pulsed particles successfully reach the microchannel plate detector, independent of the direction from which they leave the impact plate. The microchannel plate and image charge detector were used to detect ion motions in the flexible EIBT. They are both low-noise detectors. The flexible EIBT performance could be improved with modifications to the voltage gradients on the ion mirrors. The self-bunch mode of ion beam in the EIBT has better resolution than the dispersive mode of the ion beam. The difference between these two modes was due to the fact that Dr. Zajfman set up various voltage gradients on the ion mirrors. It will affect the ion various flight paths in the EIBT. We found the optimal voltage gradients in our flexible EIBT using SIMION to simulate the self-bunch mode of the ion beam. We also could change the electrode position on the Kapton film to optimize the electric field in the trap. The sensitivity of the flexible EIBT depends on the detector used and the number of the ions entering the detection region. The sensitivity of the flexible EIBT is almost the same as what Zajfman's device achieved. Our new flexible EIBT has been developed using the precision of printed circuitboard technology with a thin, flexible conductive material.

Our evaluation of the new flexible EIBT indicates that it has good resolution and sensitivity as compared to other miniaturized mass analyzers. Space charge is a big issue for miniaturized mass analyzers but the flexible EIBT still gave good resolution with no loss in sensitivity. The mass resolution of Cs^+ ions was approximately up to 1000 at 10^{-6} torr. The resolution of our miniature flexible mass analyzer is not as good as Zajfman's EIBT. The main reason is the difference in vacuum conditions. They worked at 10^{-10} torr

in their experiment. The longer mean free path gave better resolution for their device. Another reason is space charge. There are more ion-ion repulsions happening at the turn points. Nondestructive charge detection has been employed to capture the ion signals. The folding flight path in the trap provides good resolution and the possibility of small size. The electric field in the EIBT can be optimized by adjusting the potentials or the geometry of the electrodes. The ion beam shape was easier to control with the Einzel lens. All of the advantages of the EIBT could make this miniaturized mass analyzer applicable to many fields. The miniaturized flexible mass analyzer could be available for biological and chemical weapons detection, medical analysis, and outer space exploration.

References:

1. Brinckerhoff, W. B.; Cornish, T. J.; McEntire, R. W.; Cheng, A. F.; Benson, R. C., Miniature time-of-flight mass spectrometers for in situ composition studies. *Acta. Astronaut.* **2003,** *52* (2-6), 397-404.

2. Li, X.; Brinckerhoff, W. B.; Managadze, G. G.; Pugel, D. E.; Corrigan, C. M.; Doty, J. H., Laser ablation mass spectrometer (LAMS) as a standoff analyzer in space missions for airless bodies. *Int. J. Mass Spectrom.* **2012,** *323*, 63-67.

3. Hangst, J. S.; Bergsorensen, K.; Jessen, P. S.; Kristensen, M.; Molmer, K.; Nielsen, J. S.; Poulsen, O.; Schiffer, J. P.; Shi, P., Laser Cooling of Stored Ions in Astrid - a Storage Ring for Ions and Electrons. *Nucl. Instrum. Meth. B* **1992,** *68* (1-4), 17-22.

4. Bozoki, E. S.; Halama, H., Ion Related Problems for the Xls Ring. *Nucl. Instrum. Meth. A.* **1991,** *307* (2-3), 156-166.

5. Stensgaard, R., Astrid - the Aarhus Storage Ring. *Phys. Scripta.* **1988,** *T22*, 315-317.

6. Moller, S. P., ELISA, an electrostatic storage ring for atomic physics. *Nucl. Instrum. Meth. A.* **1997,** *394* (3), 281-286.

7. Matsubara, K.; Tanabe, K.; Yuasa, I.; Nakamura, H.; Tanabe, Y.; Idzu, T.; Takahashi, S.; Kimura, K., A unique and sensitive ELISA technique for typing ABH antigens in bloodstains using UEA-I lectin - The removal of detergent with a sephadex G-25 mini-column improves sensitivity. *J. Forensic Sci.* **1996,** *41* (1), 35-39.

8. Andersen, J. U.; Andersen, L. H.; Hvelplund, P.; Lapierre, A.; Moller, S. P.; Nielsen, S. B.; Pedersen, U. V.; Tomita, S., Studies of clusters and biomolecules in ELISA. *Hyperfine. Interact.* **2003,** *146* (1-4), 283-291.

9. Ring, S.; Pedersen, H. B.; Heber, O.; Rappaport, M. L.; Witte, P. D.; Bhushan, K. G.; Altstein, N.; Rudich, Y.; Sagi, I.; Zajfman, D., Fourier transform time-of flight mass spectrometry in an electrostatic ion beam trap. *Anal. Chem.* **2000,** *72* (17), 4041-4046.

10. Bredy, R.; Bernard, J.; Chen, L.; Montagne, G.; Li, B.; Martin, S., An introduction to the trapping of clusters with ion traps and electrostatic storage devices. *J. Phys. B-at. Mol. Opt.* **2009,** *42* (15).

11. Zajfman, D.; Heber, O.; VejbyChristensen, L.; BenItzhak, I.; Rappaport, M.; Fishman, R.; Dahan, M., Electrostatic bottle for long-time storage of fast ion beams. *Phys. Rev. A.* **1997,** *55* (3), R1577-R1580.

12. Dahan, M.; Fishman, R.; Heber, O.; Rappaport, M.; Altstein, N.; Zajfman, D.; van der Zande, W. J., New type of electrostatic ion trap for storage of fast ion beams. *Rev. Sci. Instrum.* **1998,** *69* (1), 76-83.

13. Pedersen, H. B.; Strasser, D.; Heber, O.; Rappaport, M. L.; Zajfman, D., Stability and loss in an ion-trap resonator. *Phys. Rev. A.* **2002,** *65* (4).

14. Zajfman, D.; Rudich, Y.; Sagi, I.; Strasser, D.; Savin, D. W.; Goldberg, S.; Rappaport, M.; Heber, O., High resolution mass spectrometry using a linear electrostatic ion beam trap. *Int. J. Mass. Spectrom.* **2003,** *229* (1-2), 55-60.

15. Rahinov, I.; Toker, Y.; Heber, O.; Strasser, D.; Rappaport, M.; Schwalm, D.; Zajfman, D., Lifetime measurements in an electrostatic ion beam trap using image charge monitoring. *Rev. Sci. Instrum.* **2012,** *83* (3).

16. Heber, O.; Witte, P. D.; Diner, A.; Bhushan, K. G.; Strasser, D.; Toker, Y.; Rappaport, M. L.; Ben-Itzhak, I.; Altstein, N.; Schwalm, D.; Wolf, A.; Zajfman, D., Electrostatic ion beam trap for electron collision studies. *Rev. Sci. Instrum.* **2005,** *76* (1).

17. Benner, W. H., A gated electrostatic ion trap to repetitiously measure the charge and *m/z* of large electrospray ions. *Anal. Chem.* **1997,** *69* (20), 4162-4168.

18. Armentrout, P. B.; Rodgers, M. T., An absolute sodium cation affinity scale: Threshold collision-induced dissociation experiments and ab initio theory. *J. Phys. Chem. A.* **2000,** *104* (11), 2238-2247.

19. Wolf, A.; Bhushan, K. G.; Ben-Itzhak, I.; Altstein, N.; Zajfman, D.; Heber, O.; Rappaport, M. L., Lifetime measurement of He- using an electrostatic ion trap. *Phys. Rev. A.* **1999,** *59* (1), 267-270.

20. Strasser, D.; Heber, O.; Goldberg, S.; Zajfman, D., Self-bunching induced by negative effective mass instability in an electrostatic ion beam trap. *J. Phys. B-at. Mol. Opt.* **2003,** *36* (5), 953-959.

21. Schmidt, H. T.; Cederquist, H.; Jensen, J.; Fardi, A., Conetrap: A compact electrostatic ion trap. *Nucl. Instrum. Meth. B* **2001,** *173* (4), 523-527.

22. Bernard, J.; Montagne, G.; Bredy, R.; Terpend-Ordaciere, B.; Bourgey, A.; Kerleroux, M.; Chen, L.; Schmidt, H. T.; Cederquist, H.; Martin, S., A "tabletop" electrostatic ion storage ring: Mini-Ring. *Rev. Sci. Instrum.* **2008,** *79* (7).

23. Ermakov, A. V.; Hinch, B. J., An electrostatic autoresonant ion trap mass spectrometer. *Rev. Sci. Instrum.* **2010,** *81* (1).

24. Rohner, U.; Whitby, J. A.; Wurz, P., A miniature laser ablation time-of-flight mass spectrometer for in situ planetary exploration. *Meas. Sci. Technol.* **2003,** *14* (12), 2159-2164.

25. Getty, S. A.; Brinckerhoff, W. B.; Cornish, T.; Ecelberger, S.; Floyd, M., Compact two-step laser time-of-flight mass spectrometer for in situ analyses of aromatic organics on planetary missions. *Rapid. Commun. Mass. Sp.* **2012,** *26* (23), 2786-2790.

26. Westmacott, G.; Frank, M.; Labov, S. E.; Benner, W. H., Using a superconducting tunnel junction detector to measure the secondary electron emission efficiency for a microchannel plate detector bombarded by large molecular ions. *Rapid. Commun. Mass. Sp.* **2000,** *14* (19), 1854-1861.

27. Schlapbach, L.; Zuttel, A., Hydrogen-storage materials for mobile applications. *Nature.* **2001,** *414* (6861), 353-358.

28. Cornish, T. J.; Ecelberger, S.; Brinckerhoff, W., Miniature time-of-flight mass spectrometer using a flexible circuitboard reflector. *Rapid. Commun. Mass. Sp* **2000,** *14* (24), 2408-2411.

29. McGuire, T. J.; Sedwick, R. J., Improved confinement in inertial electrostatic confinement for fusion space power reactors. *J. Propul Power.* **2005,** *21* (4), 697-706.

30. Attia, D.; Strasser, D.; Heber, O.; Rappaport, M. L.; Zajfman, D., Transverse kinematics of ions stored in an electrostatic ion beam trap. *Nucl. Instrum. Meth. A* **2005,** *547* (2-3), 279-286.

31. Bao, Z. N.; Rogers, J. A.; Katz, H. E., Printable organic and polymeric semiconducting materials and devices. *J. Mater. Chem.* **1999,** *9* (9), 1895-1904.

32. Odom, S. A.; Chayanupatkul, S.; Blaiszik, B. J.; Zhao, O.; Jackson, A. C.; Braun, P. V.; Sottos, N. R.; White, S. R.; Moore, J. S., A Self-healing Conductive Ink. *Adv Mater.* **2012,** *24* (19), 2578-2581.

33. Daly, R. T.; Kerby, J. D.; Austin, D. E., Electrospray charging of minerals and ices for hypervelocity impact research. *Planet Space. Sci* **2013,** *75*, 182-187.

34. Sun, Q.; Ding, L.; Gu, C. X., Modeling and optimization of dual-cylinder image current detector in electrostatic ion beam trap for mass spectrometry. *Int. J. Mass Spectrom.* **2009,** *282* (1-2), 38-44.

35. Adachi, T.; Arai, T.; Leo, K. W.; Takayama, K.; Tokuchi, A., A solid-state Marx generator driven Einzel lens chopper. *Rev. Sci. Instrum.* **2011,** *82* (8).

36. Andersen, J. U.; Hvelplund, P.; Nielsen, S. B.; Tomita, S.; Wahlgreen, H.; Moller, S. P.; Pedersen, U. V.; Forster, J. S.; Jorgensen, T. J. D., The combination of an electrospray ion source and an electrostatic storage ring for lifetime and spectroscopy experiments on biomolecules. *Rev. Sci. Instrum.* **2002,** *73* (3), 1284-1287.

37. Bhushan, K. G.; Gadkari, S. C.; Yakhmi, J. V.; Sahni, V. C., Electrostatic ion trap and Fourier transform measurements for high-resolution mass spectrometry. *Rev. Sci. Instrum.* **2007,** *78* (8).

38. Ouyang, Z.; Cooks, R. G., Miniature Mass Spectrometers. *Annu. Rev. Anal. Chem.* **2009,** *2*, 187-214.

39. Johnson, P. V.; Hodyss, R.; Tang, K. Q.; Brinckerhoff, W. B.; Smith, R. D., The laser ablation ion funnel: Sampling for in situ mass spectrometry on Mars. *Planet Space. Sci.* **2011,** *59* (5-6), 387-393.

40. Austin, D. E.; Wang, M.; Tolley, S. E.; Maas, J. D.; Hawkins, A. R.; Rockwood, A. L.; Tolley, H. D.; Lee, E. D.; Lee, M. L., Halo ion trap mass spectrometer. *Anal. Chem.* **2007,** *79* (7), 2927-2932.

41. Peng, Y.; Hansen, B. J.; Quist, H.; Zhang, Z. P.; Wang, M.; Hawkins, A. R.; Austin, D. E., Coaxial Ion Trap Mass Spectrometer: Concentric Toroidal and Quadrupolar Trapping Regions. *Anal. Chem.* **2011,** *83* (14), 5578-5584.

42. Wang, M. A.; Quist, H. E.; Hansen, B. J.; Peng, Y.; Zhang, Z. P.; Hawkins, A. R.; Rockwood, A. L.; Austin, D. E.; Lee, M. L., Performance of a Halo Ion Trap Mass Analyzer with Exit Slits for Axial Ejection. *J. Am. Soc. Mass Spectr.* **2011,** *22* (2), 369-378.